JOC The Journal of Organic Chemistry

pubs.acs.org/joc Article

Polarized, V-Shaped, and Conjoined Biscoumarins: From Lack of Dipole Moment Alignment to High Brightness

Łukasz Kielesiński, Irena Deperasińska,* Olaf Morawski, Kateryna V. Vygranenko, Erik T. Ouellette, and Daniel T. Gryko*

Cite This: J. Org. Chem. 2022, 87, 5961−5975 Read Online

ACCESS | Metrics & More | Article Recommendations | Supporting Information

ABSTRACT: Eleven conjoined coumarins possessing a chromeno[3,4-*c*]chromene-6,7-dione skeleton have been synthesized via the reaction of electron-rich phenols with esters of coumarin-3-carboxylic acids, catalyzed by either Lewis acids or 4-dimethylaminopyridine. Furthermore, Michael-type addition to angular benzo[*f*]coumarins is possible, leading to conjugated helical systems. Arrangement of the electron-donating amino groups at diverse positions on this heterocyclic skeleton makes it possible to obtain π-expanded coumarins with emission either sensitive to, or entirely independent of, solvent polarity with large Stokes shifts. Computational studies have provided a rationale for moderate solvatochromic effects unveiling the lack of collinearity of the dipole moments in the ground and excited states. Depending on the functional groups present, the obtained dyes are highly polarized with dipole moments of ∼14 D in the ground state and ∼20−25 D in the excited state. Strong emission in nonpolar solvents, in spite of the inclusion of a NO_2 group, is rationalized by the fact that the intramolecular charge transfer introduced into these molecules is strong enough to suppress intersystem crossing yet weak enough to prevent the formation of dark twisted intramolecular charge transfer states. Photochemical transformation of the dye possessing a chromeno[3,4-*c*]pyridine-4,5-dione scaffold led to the formation of a spirocyclic benzo[*g*]coumarin.

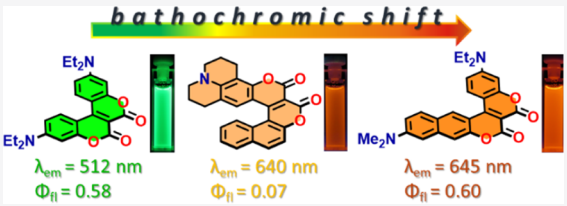

INTRODUCTION

Although coumarins were first synthesized almost 150 years ago,[1] they are still of interest to many researchers worldwide. This fact is mainly related to their very wide range of applications. Many groups of coumarins exhibit biological activity, including anti-inflammatory, antifungal, antibacterial, or dermal photosensitizing properties, that make them useful in the medicinal and pharmaceutical industries.[2−4] In addition to the features associated with their bioactivity, coumarins possess very interesting photophysical properties.[5−7] These compounds are highly desirable for applications in solar cells,[8] organic light-emitting diodes,[9] and laser dyes[10] due to their relatively simple, easily tunable structures, along with their high fluorescence quantum efficiencies, long decay times, and large Stokes shifts. Modification of the molecular structure of coumarins by extending the π-electron system strongly influences their electronic spectra. Consequently, appropriately substituted π-expanded coumarins exhibiting bathochromic shifts in the absorption and emission spectra are increasingly used in biological imaging, thanks to the deeper tissue penetration depth of this spectral region (Figure 1).[11] A significant portion of research has been dedicated to fluorescent benzo[*g*]coumarin-based probes applicable for two-photon microscopy.[12] Another interesting feature of π-expanded coumarins is the opportunity to apply them in the construction of new classes of optoelectronic materials.[13]

In the last few years, empowered by synthetic advances, previously unknown π-expanded coumarins have been explored, including those exhibiting a helical structure (Figure 1).[14] Among the significant number of reported skeletons, coumarin[3,4-*c*]coumarins (chromeno[3,4-*c*]chromene-6,7-diones), that is, V-shaped conjoined biscoumarins, have attracted the most attention. Although known since 1984,[15−17] they have only recently experienced a renaissance[18−22] due to more straightforward synthetic methods becoming available.[23,24] Inspired by straightforward and programmable preparation of coumarin[3,4-*c*]coumarin, we reasoned that modulation of photophysical properties can be achieved via employing π-expanded coumarins as building blocks in this two-component reaction. The simultaneous goal of this study was to design V-shaped biscoumarins with large dipole moments exceeding 10 debye, a value being in the ground electronic state usually an upper limit for molecules with large solvatochromism or showing dual emission as a result of twisted intramolecular charge transfer.[25−29] This can be intuitively understood as the polarized moieties of a conjoined molecule contributing to the

Received: January 31, 2022
Published: April 12, 2022

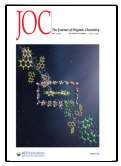

https://doi.org/10.1021/acs.joc.2c00232
J. Org. Chem. 2022, 87, 5961−5975

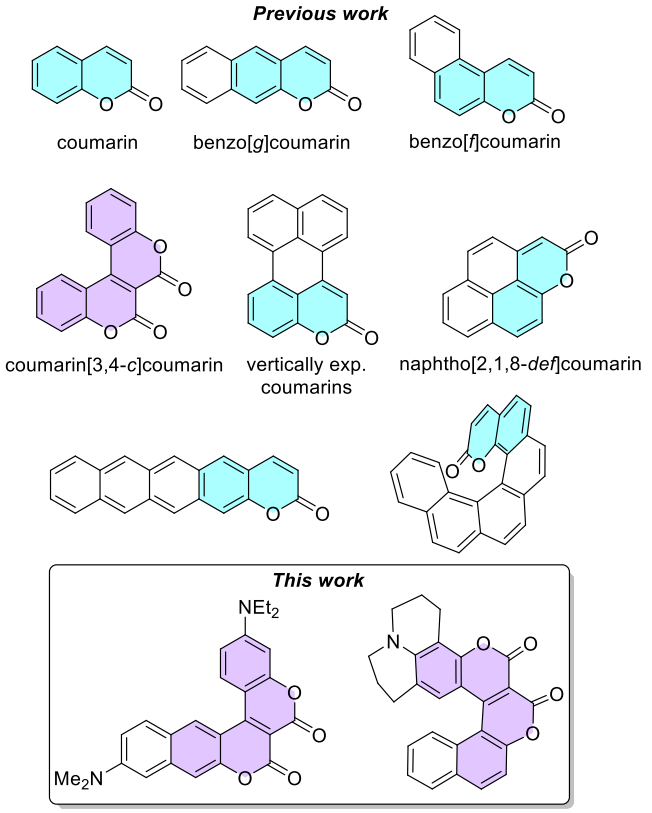

Figure 1. Structures of various π-expanded coumarins.

total dipole of the V-shaped structure (two vectors $\overrightarrow{V_1}$ and $\overrightarrow{V_2}$ add up to the resultant $\overrightarrow{V_3}$). Such a description is, however, very oversimplified because it completely ignores the electronic coupling within the conjoined system and reduces interactions with Coulombic forces, which are further truncated to the dipole−dipole term only. At short distances, the multipole expansion is not exact even if it takes several orders, so the simple picture with dipoles is not valid. Therefore, a careful experimental study and a detailed theoretical exploration with quantum chemistry calculations are required for understanding the photophysics and optical properties of the V-shaped coumarins.

RESULTS AND DISCUSSION

Design and Synthesis. Harnessing the propensity of strongly polarized benzo[*g*]coumarins to have large dipole moments originating from linearly extended conjugation was chosen as one of the key strategies to achieve our goal. We hypothesized that replacing one coumarin unit in a chromeno-[3,4-*c*]chromene-6,7-dione scaffold with benzo[*g*]coumarin would lead to conjoined coumarins possessing bathochromically shifted emission and large dipole moments. Simultaneously, starting from benzo[*f*]coumarin may deliver curved coumarins analogous to [5]helicene. Our synthetic strategy capitalized on the fact that coumarins with an ester group in the 3 position form V-shaped condensation products when heated with reactive phenols or amidines in the presence of a catalyst, such as Lewis acids or some types of organic bases.[23,30] By virtue of the electronic demands of these reactions, the nucleophilic partner has to possess two electron-donating groups. Thus, the structural possibilities leading to various electronic configurations have to be realized by varying the electrophilic substrate, that is, coumarin. The project started from the synthesis of dyes **3** and **5** possessing a C_{2v}-symmetric scaffold with two amino groups present, dye **7** bearing a NO_2 group and dye **8**. In all cases, the motivation lied in having conjoined biscoumarins with various arrangements of electron-donating and -withdrawing groups for comparison of photophysical properties. Compound **3** was obtained by the reaction of methyl 7-(diethylamino)-2-oxochromene-3-carboxylate (**1**) and 3-diethylaminophenol (**2**) in the presence of $AlCl_3$ as a catalyst. Despite the optimization studies carried out (type of catalyst, reaction temperature, and time), after 24 h at 140 °C, the conversion was still low and the desired compound was isolated in only 7% yield (Scheme 1).

Scheme 1. Synthesis of Biscoumarins 3 and 5

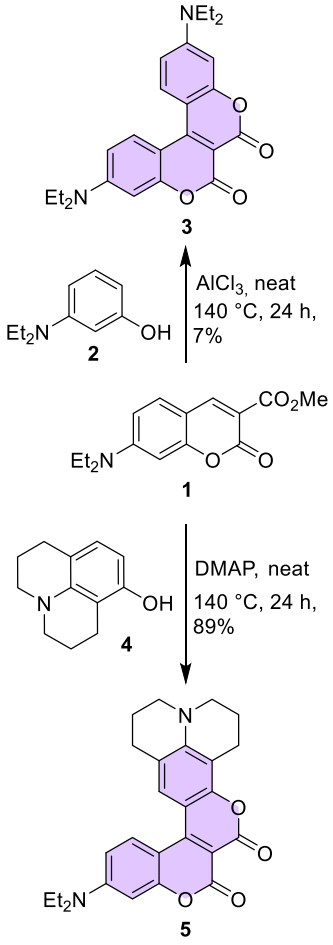

The low yield prompted us to attempt to identify side-products in this reaction. Unfortunately, however, these attempts were futile, mostly because the presence of multiple, unstable side-products, which could not be isolated in a pure state. Mass spectrometry of combined fractions containing side-products have revealed that there are no regioisomeric conjoined coumarins present. On the other hand, biscoumarin **5** was obtained in significantly higher yield simply by changing the catalyst to *N*,*N*-dimethylpyridine-4-amine (DMAP) (Scheme 1). The presence of only one reactive position in the structure of 8-hydroxyjulolidine has plausibly the biggest impact on this yields' difference. Subsequently, we synthesized biscoumarin **8**, which differs by the position of an amino group in one of the

https://doi.org/10.1021/acs.joc.2c00232
J. Org. Chem. 2022, 87, 5961−5975

coumarin subunits. We wanted to investigate how the location of the donor substituent influences the photophysical properties when compared to biscoumarins substituted in the 7 position. We were curious if a similar behavior would be observed to that of simple 6-amino and 7-aminocoumarins.[31] Unfortunately, the reaction of 6-aminocoumarin derivatives with appropriate phenols was low-yielding and many side-products were observed.

Therefore, we started the synthesis of dyes **7** and **8** by obtaining compound **6**, which was subsequently reacted with 3-diethylaminophenol (**2**) in the presence of indium triflate ($In(OTf)_3$) (Scheme 2). The reduction of the nitro group with tin(II) chloride led to the desired coumarin **8** in good overall yield.[32]

Scheme 2. Synthesis of Biscoumarins 7 and 8

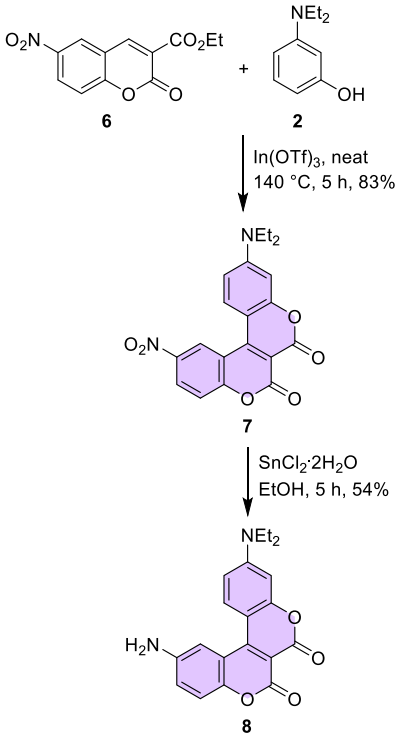

We then turned our attention to benzo[*g*]coumarins as starting materials.[12,33] We started the synthesis by preparation of the appropriately substituted benzo[*g*]coumarin **9** using methodology developed by Ahn and co-workers.[34] In the crucial step, we carried out the reaction with 3-diethylaminophenol (**2**) in the presence of different catalysts, such as $In(OTf)_3$, $Al(OTf)_3$, $AlCl_3$, $FeCl_3$, and others Lewis acids, but the best results were obtained with DMAP (Scheme 3).

Next, this approach was applied to a broader group of substrates. Using the same set of conditions and 8-hydroxyjulolidine (**4**), 3-(ethylamino)-*p*-cresol, and 7-hydroxy-1,2,3,4-tetrahydroquinoline, we synthesized compounds **11**, **12**, and **13** in 39, 36, and 41% yields, respectively (Figure 2). The yields in the range of 30−40% were related to the formation of many side-products, which were observed during the reaction. It is noteworthy that conversion of aminophenol was 100% in all these cases.

These results encouraged us to apply this strategy to benzo[*f*]coumarins as electrophilic partners, which should deliver conjoined coumarins bearing the [5]helicene motif. We expected that it would be a more difficult challenge, mainly due to a greater steric hindrance. However, coumarin **14** in reaction with 8-hydroxyjulolidine (**4**) gave coumarin **15** in acceptable yield (Scheme 4).

Scheme 3. Synthesis of Biscoumarin 10

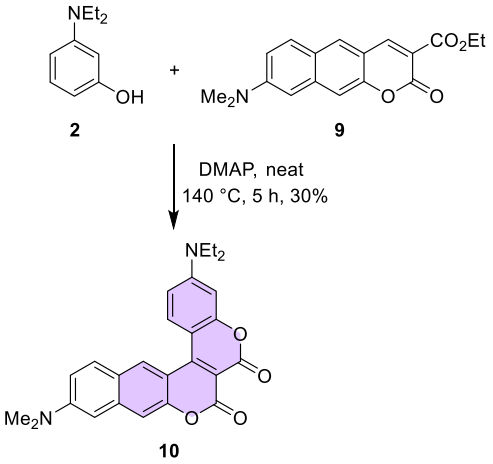

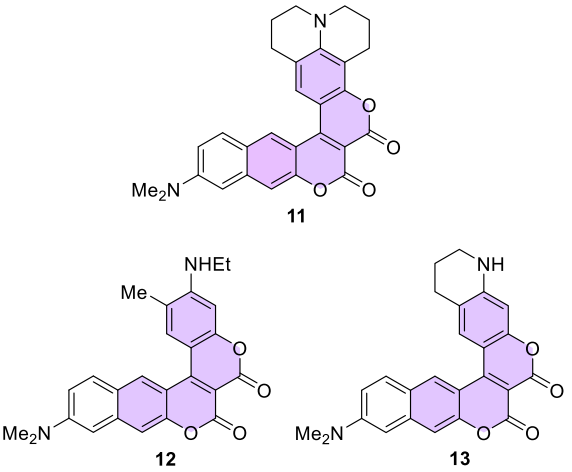

Figure 2. Structures of biscoumarins **11**−**13**.

Scheme 4. Synthesis of Biscoumarin 15

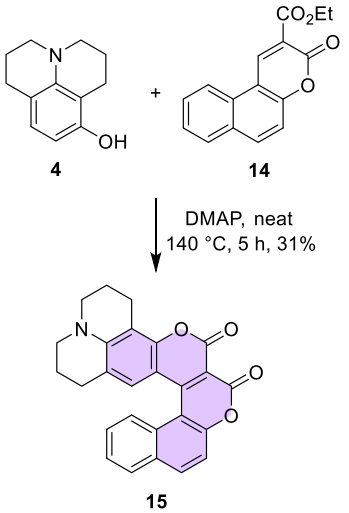

https://doi.org/10.1021/acs.joc.2c00232
J. Org. Chem. 2022, 87, 5961−5975

By analogy, coumarins **16** and **17** were synthesized using appropriate phenols (Figure 3), although the yields were lower

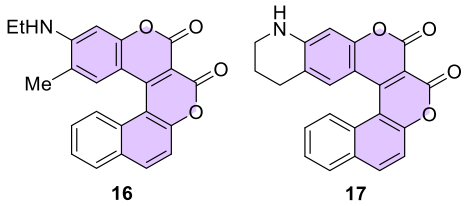

16 **17**

Figure 3. Structures of biscoumarins **16** and **17**.

(18% in both cases) when compared to molecules based on the benzo[*g*]coumarin core. We also carried out the reaction with 3-diethylaminophenol (**2**), but in this case we observed only trace amounts of product, regardless of the catalyst used, which might be a result of the larger steric hindrance in relation to compound **10**.

Finally, we attempted the cyclocondensation of benzocoumarins with 1,8-diazabicyclo[5.4.0]undec-8-ene (DBU) and 1,5-diazabicyclo[4.3.0]non-5-ene (DBN) employing the conditions developed a few years ago for the reaction of amidines with substituted coumarins.[24] π-Expanded coumarins **18** and **19** were successfully prepared, although the reaction with DBU was longer and the yield of the product was slightly lower (59%) than in the case of reaction with DBN (Scheme 5). This is probably related to a smaller steric hindrance observed for the compound with five membered rings at the periphery of the system.

Scheme 5. Synthesis of Compounds 18 and 19

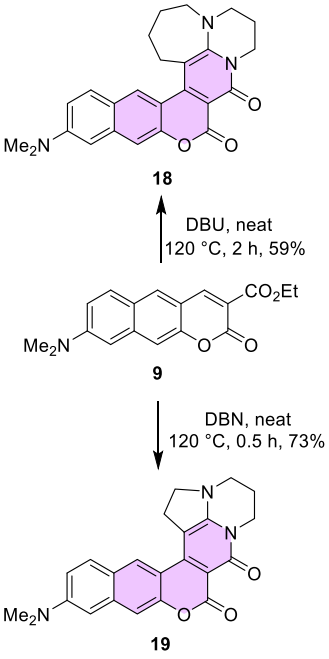

The same conditions applied for benzo[*f*]coumarin **14** in reaction with DBN led to the product **20** in a slightly lower yield (38%) (Scheme 6), whereas in reaction with DBU only traces of desired product were observed. In both cases, the result was very likely due to the even larger steric hindrance caused by the seven membered ring.

Scheme 6. Synthesis of Compound 20

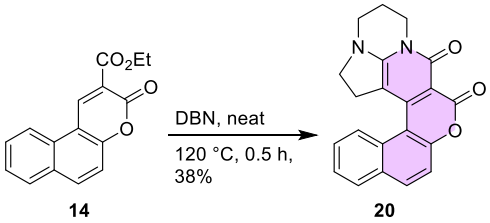

Additionally, an interesting stability phenomenon was observed for compound **19**. We noticed that this molecule dissolved in dichloromethane (DCM) exposed to air and sunlight is transformed into many fluorescent products. Among them, from the reaction mixture, compound **21** could be isolated, but the yield was only 18% (Scheme 7). The structure of this compound was fully confirmed by X-ray analysis (Figure 4) as well as by NMR spectroscopy.

Scheme 7. Light-Induced Formation of Spiro-coumarin 21

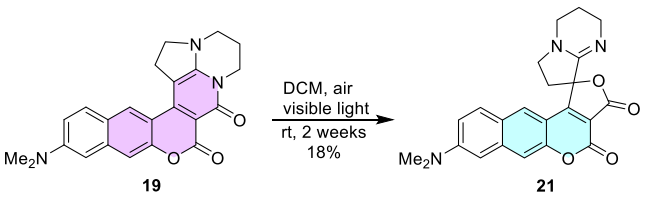

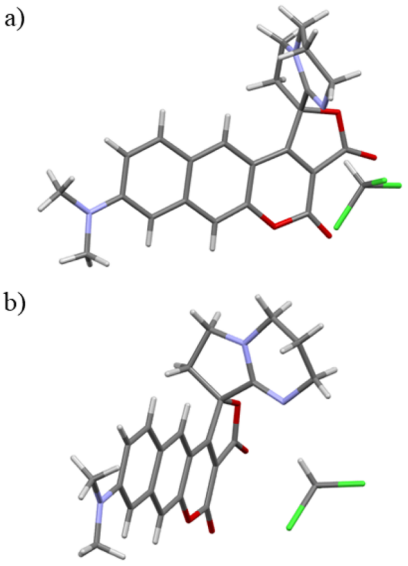

Figure 4. X-ray structure of spiro-coumarin **21**: (a) front view; (b) side view.

Single-Crystal X-ray Diffraction Studies. Spiro-coumarin **21** was crystallized by slow diffusion of hexane into chloroform. The orange shards of 0.04 mm × 0.04 mm × 0.04 mm size were appropriate for X-ray analysis. The crystallographic structure of compound **21** is presented in Figure 4. The crystal belongs to the $P2_1/n$ space group. As shown in Figures 4 and S2, the part of molecule with the coumarin moiety fused with the five-membered lactone ring is planar, while the amidine moiety is positioned in a perpendicular arrangement. The dihedral angle between the coumarin core and the plane of the DBN ring is close to 90° (Figure S2). The molecule exhibits an antiparallel packing in the unit cell

https://doi.org/10.1021/acs.joc.2c00232
J. Org. Chem. 2022, 87, 5961−5975

Table 1. Spectroscopic Properties of Dyes 3, 5, 7, 8, 10−13, and 15−21 Obtained in Toluene, DCM, and ACN

comp.	solvent	λ_{abs}^{max} [nm]	λ_{em}^{max} [nm]	ε [M^{-1}cm^{-1}]	Stokes shift [cm^{-1}]	Φ_F[a]	τ_{aver} [ns]	k_r[b] [ns^{-1}]	k_{nr}[c] [ns^{-1}]
3	toluene	419	473	51 500	2700	0.36	1.45	0.248	0.441
	DCM	453	494	60 900	1800	0.43	1.87	0.230	0.305
		422		56 000					
	ACN	451	512	56 200	2600	0.58	2.59	0.224	0.162
		420		52 700					
5	toluene	449	500	42 500	2300	0.37	2.06	0.180	0.306
		421		44 500					
	DCM	467	525	55 200	2400	0.44	3.96	0.111	0.141
		424		47 300					
	ACN	466	546	49 500	3100	0.83	4.36	0.190	0.039
		422		42 100					
7	toluene	469	532	24 900	2500	0.71	6.55	0.108	0.044
	DCM	480	560	31 100	3000	0.22	0.82	0.268	0.951
	ACN	471	576	29 000	3900	0.0007	0.06	0.012	16.66
8	toluene	441	557	27 100	4700	0.05	1.27	0.039	0.748
	DCM	459	545	35 500	3400	0.015	3.33	0.005	0.296
	ACN	451	647	30 200	6700	0.006	0.92	0.007	1.080
10	toluene	445	547	45 900	4200	0.68	1.45	0.469	0.221
	DCM	456	597	53 600	5200	0.76	5.17	0.147	0.046
	ACN	453	645	45 400	6600	0.60	5.16	0.116	0.078
11	toluene	454	544		3600	0.41	1.24	0.331	0.476
	DCM	498	586	46 500	3000	0.61	3.78	0.161	0.103
		466		48 900					
	ACN	494	634		4500	0.53	4.74	0.112	0.099
		465							
12	toluene	437	546		4600	0.59	3.69	0.160	0.111
	DCM	443	599	38 400	5900	0.65	5.58	0.116	0.063
	ACN	445	648	70 000	7000	0.63	4.82	0.131	0.077
13	toluene	443	545		4200	0.53	3.40	0.156	0.138
	DCM	449	597	45 800	5500	0.76	5.51	0.138	0.044
	ACN	451	645		6700	0.45	4.60	0.098	0.120
15	toluene	478	576	23 700	3600	0.56	5.59	0.100	0.079
		402		10 200					
		381		9100					
	DCM	495	607	33 400	3700	0.29	4.14	0.070	0.171
		401		12 800					
		381		12 000					
	ACN	491	640	25 100	4700	0.07	1.22	0.057	0.762
		399		9200					
		381		8800					
16	toluene	437	540		4400	0.23	2.23	0.103	0.345
	DCM	451	556	25 800	4200	0.27	3.41	0.079	0.214
		404		18 300					
	ACN	453	593	24 300	5200	0.14	2.18	0.064	0.394
		401		15 100					
17	toluene	449	549		4100	0.29	3.06	0.095	0.232
		404							
	DCM	462	567	24 600	4000	0.36	3.88	0.093	0.165
		404		14 400					
	ACN	463	597	24 500	4800	0.10	1.45	0.069	0.621
		400		12 500					
18	toluene	407	529		5700	0.015	0.35	0.043	2.814
	DCM	410	517	32 100	5000	0.04	0.50	0.080	1.920
	ACN	408	544	26 300	6100	0.03	0.49	0.061	1.980
19	toluene								
	DCM	429	488		2800	0.64	2.32	0.276	0.155
		405							
	ACN	429	517		4000	0.67	3.21	0.209	0.103
		404							
20	toluene	414	516		4800	0.08	1.86	0.043	0.495
		363							

https://doi.org/10.1021/acs.joc.2c00232
J. Org. Chem. 2022, 87, 5961−5975

Table 1. continued

comp.	solvent	λ_{abs}^{max} [nm]	λ_{em}^{max} [nm]	ε [M^{-1}cm^{-1}]	Stokes shift [cm^{-1}]	Φ_F[a]	τ_{aver} [ns]	k_r[b] [ns^{-1}]	k_{nr}[c] [ns^{-1}]
		318							
	DCM	409	520	11 100	5200	0.09	2.17	0.041	0.419
		359		9800					
		318		22 400					
	ACN	409	537	9600	5800	0.08	2.44	0.033	0.377
		355		8400					
		316		21 000					
21	toluene	449	525		3200	0.71	5.10	0.139	0.057
		327							
	DCM	476	574	26 200	3600	0.74	5.50	0.135	0.047
		332		14 300					
	ACN	468	604	23 300	4800	0.78	5.60	0.139	0.039
		329		12 000					

[a]Fluorescence quantum yield measured using an integrating sphere. [b]$k_r = \Phi_F/\tau_{aver}$. [c]$k_{nr} = 1/\tau_{aver} - k_r$.

(Figure S1). The distance between the planes of the coumarin moiety of the two neighboring molecules is around 3.8 Å.

Photophysical results. Photophysical properties were measured for compounds **3**, **5**, **7**, **8**, **10**−**13**, and **15**−**21** in nonpolar toluene (dielectric constant ε = 2.38), moderately polar DCM (ε = 8.93), and polar acetonitrile (ACN, ε = 38.8). Absorption and normalized fluorescence spectra for all molecules are presented in Figure S4 and Table 1. Compounds **3** and **5** possessing two electron-donating groups exhibited absorption and emission spectra in the range of 419−467 and 473−546 nm, respectively, which mostly correspond to the properties of other biscoumarin derivatives.[23] Coumarin **7** bearing a NO_2 group, as well as compound **8** possessing NH_2 group, have bathochromically shifted spectra compared to previous molecules, which is particularly prominent in the case of emission (Figure S4).

Fluorescence spectra of the π-expanded conjoined coumarins containing benzo[*g*]- and benzo[*f*]coumarin cores are significantly more red-shifted than the spectra of simple V-shaped coumarins **3** and **5** (Figures 5 and S4) and are characterized by large Stokes shifts in the range of 3000−7000 cm^{-1} (Table 1). Additionally, the fluorescence spectra show solvatochromism when going from nonpolar to polar solvents,

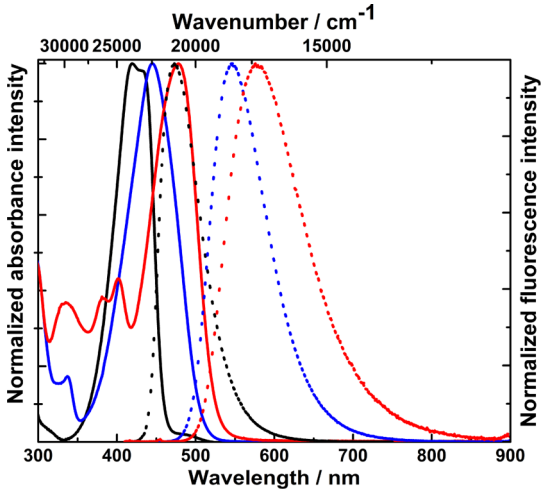

Figure 5. Absorption (solid line) and emission (dot line) spectra of dyes **3** (black, excited at 382 nm), **10** (blue, excited at 400 nm), and **15** (red, excited at 400 nm) measured in toluene.

thereby suggesting that these compounds have large dipole moments in the excited state. For compounds **18**, **19**, and **20**, the location of absorption bands was very similar to those of other molecules described in the literature.[24,35] Their emission spectra, however, are significantly shifted toward lower energy, which can be related to the strong electronic coupling present in the large π-expanded structure.

Most of the conjoined coumarins are strongly fluorescent in all solvents;, however, a difference in behavior is observed for some of them. Fluorescence quantum yields (Φ_F) for compounds **3** and **5** are larger in polar solvents than in nonpolar solvents, where the nonradiative process rate k_{nr} increases (Table 1). This points to stabilization of the emissive S_1 state in a polar environment. Compounds **7** and **8** exhibit low Φ_F in all solvents, which suggests an emission from a dark state giving a small value of the radiative rate, k_r, and a large radiationless rate, k_{nr} (Table 1). Conjoined coumarins **10**−**13** possess fluorescence quantum yields in the range 0.41−0.76, while compounds **15**, **16**, and **17** are in the range from 0.07 to 0.56. A decrease of Φ_F with the increase of solvent polarity was observed for most of these compounds (Table 1). Compound **18** exhibited very low Φ_F (0.015−0.04), which could be related to the presence of a more flexible seven membered ring compared to **19**, which had a large Φ_F (0.64−0.67) and more rigid structure. Despite the fact that compound **20** possesses the same five-membered ring structure as molecule **19**, its fluorescence quantum yield is rather low (Table 1). This difference originates from the lack of an electron-donating group in its structure. Most of the conjoined coumarins have a one-exponential fluorescence decay profile with lifetimes ranging from 1 to 6 ns (Table S2). In a few cases, two component exponential decay is observed, which could be related to the presence of additional CT states. The values of the second fluorescence lifetime, τ_2, were significantly longer indicating that the CT state lives longer than the LE state (Table S2).

Having this large library in hand, an interesting comparison can be made. Addition of a second amino group, that is, transforming the original chromeno[3,4-*c*]chromene-6,7-diones into conjoined coumarins possessing pure C_{2v} symmetry has a negligible hypsochromic effect on λ_{abs} (463 nm → 453 nm) and λ_{em} (528 nm → 494 nm). At the same time, however, it does influence Φ_F, which is smaller for symmetric derivatives **3** and **5** although this increases and not decreases in polar solvents.

https://doi.org/10.1021/acs.joc.2c00232
J. Org. Chem. 2022, 87, 5961−5975

The second interesting comparison is related to coumarins **8** versus **3** (Figure 6). It is well-known that moving the amino

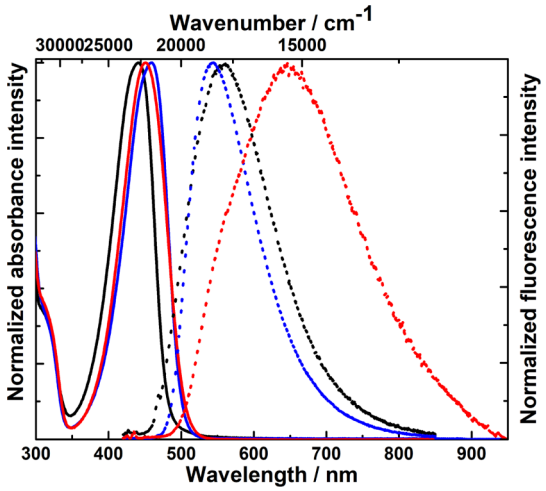

Figure 6. Absorption (solid line) and emission (dotted line) spectra of compound **8** (excited at 410 nm) measured in toluene (black), DCM (blue), and ACN (red).

group from position 6 to position 7 has a profound effect on coumarin photophysical properties leading to a bathochromic shift of emission and a strong decrease in fluorescence quantum yield.[6b,c,31e] Combining 6-aminocoumarin with 7-aminocoumarin moieties in one dye leads to perplexing questions about "what will prevail". As it turns out, the presence of an amino group at position 6 has a profound effect on decreasing the fluorescence quantum yield to 0.05 in nonpolar solvents and moves the emission in polar solvents to approx. 650 nm.

Breakthrough work by Ahn and co-workers has revealed that 8-dialkylamino-3-carboxymethyl-benzo[*g*]coumarin has absorption and emission markedly bathochromically shifted versus the electronically analogous 7-dialkylamino-3-carboxymethyl-coumarin, from 453 to 565 nm (in DCM), respectively.[12,34] The direct comparison of dyes **3** and **10** shown that although λ_{abs} values are only slightly bathochromically shifted, the emission is red-shifted by 70−150 nm, depending on the solvent (Figure 5). At the same time in contrast to many classical coumarins, the fluorescence intensity neither decreases nor increases in polar solvents.

The variations of photophysical properties within the group of conjoined coumarins **10**, **11**, **13**, and **15**, all possessing the same core, but differing in the nature of the amino substituent at the coumarin moiety, are negligible.

The fundamental difference between helical conjoined coumarins **17**−**19** and their analogs derived from benzo[*g*]-coumarins is obvious, that is, a minimal hypsochromic shift of both absorption and emission in toluene, but a larger in the case of ACN. The emission intensity is smaller, however, and it decreases sharply while moving to solvents with larger ε, although one can notice that dye **16** has a less sharp decrease in Φ_F in a polar solvent, which resembles earlier observations by Ahn[36] as well as by Gryko and Sobolewski showing that coumarins possessing an ethylamino group at position 7 are fluorescent in polar environments.[37]

Replacing the second coumarin moiety with a lactam shifts λ_{abs} of the resulting benzo[*g*]coumarins **18** and **19** hypsochromically (Figure 7). Similar to earlier observations

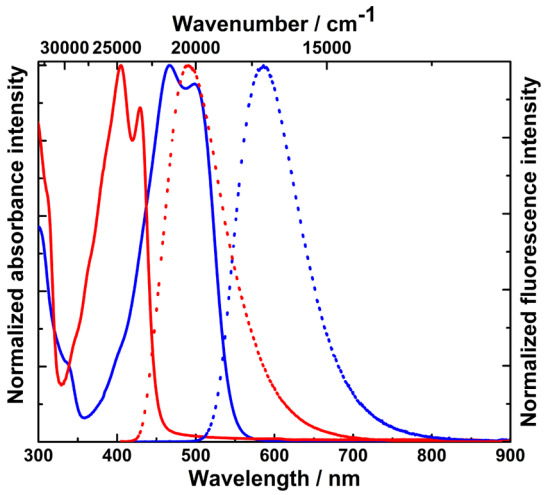

Figure 7. Absorption (solid line) and emission (dotted line) spectra of dyes **11** (blue, excited at 410 nm) and **19** (red, excited at 395 nm) measured in DCM.

performed for an analogous series possessing five-membered and seven-membered rings,[24] emission of **19** is strong, whereas that of **18** is weak in solutions regardless of solvents' polarity.

10-(Diethylamino)-2-nitro-chromeno[3,4-*c*]chromene-6,7-dione (**7**) possessing a NO_2 group represents a very special case due to a recent surge of interest in fluorescent nitroaromatics.[38] It is worth noting that fluorescence of this dye in toluene reaches 0.71 and decreases sharply in polar solvents (Table 1). This is in strong contrast to a previously described analog 3-(diethylamino)-10-nitro-chromeno[3,4-*c*]-chromene-6,7-dione, which had undetectable fluorescence.[23] The only difference between these two structures is the position of the NO_2 group.

Interesting photophysical properties are displayed by compound **21**. The maxima of absorption and emission spectra are in the range of 449−476 and 525−604 nm, respectively (Figure S4 and Table 1). The position of absorption bands is very similar to those of compounds **10**−**13** as well as molecules with a helical structure and a benzo[*f*]coumarin core. Although the emission bands of spiro-coumarin **21** are slightly hypsochromically shifted (Table 1), the opposite situation was observed compared to compounds **19** and **20** with the DBN moiety. In this case, both the absorption and emission spectra of spiro-coumarin **21** were significantly red-shifted (Table 1). Comparing molecule **19**, which is the direct precursor for spiro-coumarin **21**, the differences in the location of the absorption and emission maxima are 47 and 86 nm in DCM, respectively (Figure 8).

Spiro-coumarin **21**, like most of the presented conjoined V-shaped coumarins in this work, is also a strongly luminescent molecule. In all three solvents, Φ_F is in the range of 0.71−0.78. We see that in this case, the solvent polarity does not significantly influence these values. The large Φ_F correlates with relatively long lifetimes similar to the case of compound **19**. The radiative rate constant k_r is from 2.4 to 3.5 times larger than the nonradiative rate constant k_{nr}, which suggests that radiative processes dominate (Table 1).

Computational results. Calculations were performed using the Gaussian 16 package at the density functional theory (DFT and TDDFT) level with the PCM procedure for description of solvent effects.[39] The optimization of molecular structures in the ground (S_0) and electronic excited (S_1) states

https://doi.org/10.1021/acs.joc.2c00232
J. Org. Chem. 2022, 87, 5961−5975

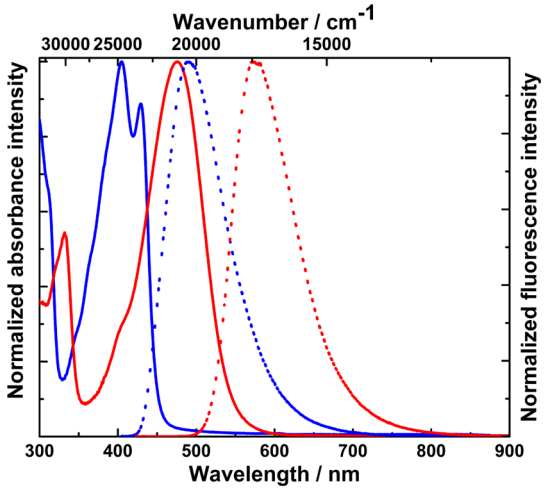

Figure 8. Absorption (solid line) and emission (dotted line) spectra of dyes **19** (blue, excited at 395 nm) and **21** (red, excited at 420 nm) measured in DCM.

was conducted with B3LYP and M06 functionals. The optimization has been confirmed by positive values of all calculated vibrational frequencies.

Calculations of the energy of electronic transitions $S_0 \rightarrow S_1$ and $S_1 \rightarrow S_0$ and the corresponding oscillator strengths for the considered coumarins in three solvents were performed to get insights into the photophysical processes. The calculations were preceded by the optimization of coumarin structures in both the S_0 and S_1 states. The results of these extensive calculations by the TD B3LYP/6-31G (d,p) method are summarized in Table S3 in the Supporting Information. In the same Table S3, the results of the calculations with the M06 functional can also be found due to the need for caution with the B3LYP functional known for its limitations. The use of the M06 functional leads to slightly higher transition energies, and in three cases (conjoined coumarins **7**, **8**, and **18**) it turned out to be more beneficial, but it did not change the conclusions resulting from the other calculations. The calculated oscillator strength and transition energy for the $S_1 \rightarrow S_0$ transition were used to estimate the radiative transition rate constants k_r. The calculated transition energies for absorption and fluorescence, as well as the radiative constants (Table S3) were correlated with the relevant experimental data (taken from Table 1), as shown in Figures S5−S7 in the Supporting Information. Most of the calculated transition energies are correlated within tolerable ±0.15 eV accuracy.[40] Also, most of the values of the estimated radiative transition rate constants correlate well with the experiment. However, the correlation between the calculated experimental values for two coumarins **7** and **18** is not acceptable. Coumarin **7** in a nonpolar environment is characterized by high fluorescence efficiency, while the oscillator strength calculated for it is low. The opposite problem occurs with coumarin **18**. Thus, in both cases it was necessary to search for other (than those originally optimized) stable forms in the excited state.

General Outlook. The conjoined coumarins can be considered in terms of two coumarin cores, sharing one common central bond with coumarin **11** as an example (Figure S8). Steric interactions between the two moieties make them nonplanar structures. Characteristic features of these are large values of dipole moments. Results of the calculations presented in Table 2 reveal that all conjoined biscoumarins are highly polarized in the ground state and their dipole moments (≈14 D) are much larger than that of benzo[*g*]coumarin **9** (7 D)[33] or **CoumMono** (≈10 D)[37] structurally analogous to coumarins used for laser dyes and other purposes.[41] In the excited state, the dipole moment increases to values around 20 D or larger (again larger than **CoumMono**[37] and comparable to dye **9**,[33] Table 2) and the optical transition is fully allowed in absorption and in emission, suggesting possible large fluorescence quantum yield, which is indeed observed (Table 1). Interestingly, the observed solvatochromic effects are rather moderate considering the high dipole moment. The reason is the noncollinearity of the dipole moments in the ground and excited states, with an angle of ≈30° between them (Table 2). The reason for this noncollinearity is the specific character of the electronic excitation in the conjoined V-shaped coumarins.

Table 2. Calculated (B3LYP) Values of Electronic Transition Energies (E_{abs} and E_{em}), Oscillator Strengths (f), and Dipole Moments of Conjoined Coumarins in Toluene: μ_g in the Ground State (S_0) and μ_e in the Excited (S_1) State[a]

	S_0 state			S_1 state			S_1 vs S_0		
comp.	E_{abs} [nm]	f	$\lvert\mu_g\rvert$ [D]	E_{em} [nm]	f	$\lvert\mu_e\rvert$ [D]	α [deg]	$\lvert\mu_e\rvert - \lvert\mu_g\rvert$ [D]	$\lvert\mu_e - \mu_g\rvert$ [D]
3	412.5	0.8229	14.85	451.9	0.5716	19.32	29.9	4.47	3.52
5	425.8	0.7251	14.97	478.6	0.4891	19.48	30.5	4.51	2.65
7	458.3	0.0650	10.37						
8	442.1	0.2241	14.65	597.7	0.1038	19.24	30.0	4.59	3.76
10	476.1	0.5061	16.16	542.7	0.3056	24.17	33.5	8.01	3.40
11	475.7	0.5629	16.10	539.0	0.3311	23.90	33.3	7.80	3.82
12	472.5	0.4919	16.29	543.4	0.2879	24.18	32.7	8.17	3.90
13	473.6	0.4783	16.54	545.1	0.2809	24.45	32.1	7.91	3.88
15	454.6	0.4179	14.03	583.8	0.2165	19.94	30.9	5.91	3.00
16	424.4	0.4085	14.13	547.2	0.1994	19.12	29.6	4.99	3.28
17	430.9	0.3985	14.41	554.9	0.1979	19.33	28.5	4.93	3.37
18	418.0	0.5089	12.94						
19	405.3	0.5723	13.51	459.3	0.3772	19.51	38.1	6.00	3.38
20	399.7	0.1303	12.26	511.8	0.0705	15.91	37.7	3.65	3.23

[a] α is the angle between μ_g and μ_e; $\lvert\mu_e\rvert - \lvert\mu_g\rvert$ is the difference in scalar values of dipole moments; $\lvert\mu_e - \mu_g\rvert$ is the value of the vector difference between both vectors—this is the factor that determines the size of the solvatochromic effect, as it is known from the theory of the Lippert−Mataga solvent effect.[42] Lippert−Mataga expressions are recalled in the Supporting Information.

https://doi.org/10.1021/acs.joc.2c00232
J. Org. Chem. 2022, 87, 5961−5975

Frontier orbitals of conjoined coumarins share common features: their HOMOs are located on one of the components, while their LUMOs are shared. This is shown in the molecular energy diagrams for two coumarins **11** and **15** in Figure 9.

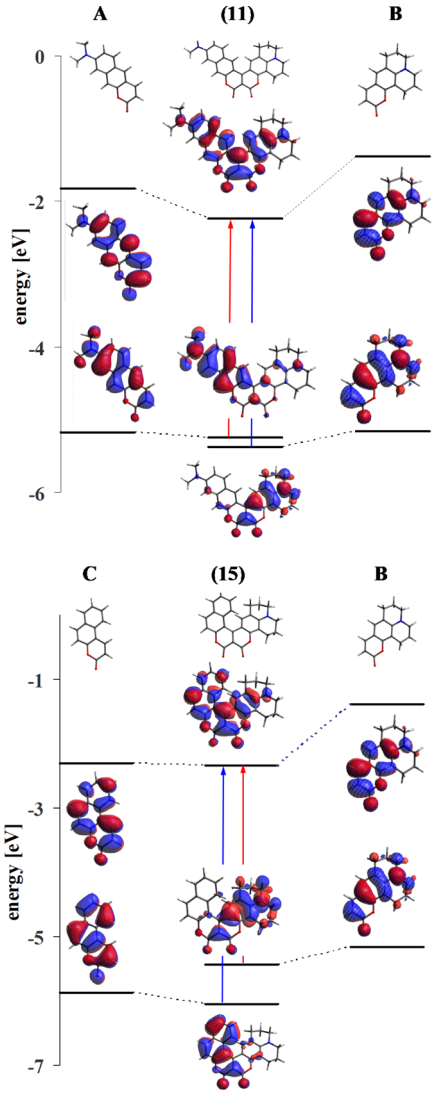

Figure 9. Molecular orbital energy diagrams with frontier orbitals of conjoined coumarins **11** and **15** and the character of the $S_0 \rightarrow S_1$ transition (marked in red) and $S_0 \rightarrow S_2$.

Hence, the HOMO → LUMO transition is partially located on the components on which the HOMO is located, and partially it is a CT transition to the second component. Consequently, the electronic transition $S_0 \rightarrow S_1$ in conjoined coumarins is characterized by transition moment vectors directed from one coumarin moiety to the second coumarin moiety. As a result, in the excited state of the conjoined coumarins, the direction of the dipole moment changes compared to the ground state, as shown in Table 2.

One of the components of both depicted conjoined coumarins is the same coumarin core, labeled B. The couplings between the HOMO components are not large and in both conjoined coumarins, they remain practically localized to one of the components. Due to the difference in ionization potential between these parts, in the A−B combination, the HOMO of coumarin **11** is located on A, while in the B−C combination, the HOMO of dye **15** is located on B. Therefore, the $S_0 \rightarrow S_1$ transition in coumarin **11** is a transition partially located on A, and it takes place as a partial CT transition from A to B. The $S_0 \rightarrow S_1$ transition in dye **15**, however, is partially located on B and is partially a CT transition from B to C. Due to the relatively small fission of HOMO and HOMO − 1 (each located on one of the coumarin moieties), the $S_0 \rightarrow S_1$ and $S_0 \rightarrow S_2$ transitions have similar energies (which is confirmed by experiment).

The oscillator strengths (Table 2 and Table S3) in almost all conjoined coumarins are large with values typical for fully allowed optical transitions. Oscillator strengths for the conjoined V-shaped coumarins are larger than for their constituent parts (Table S4), revealing strong coupling in the extended π-electron system. This is also manifested by significant lowering of the excited state energy transitions in the conjoined coumarins occurring at energies lower than in a single component molecule. In the large group of coumarins tested in this work, there were also cases that displayed properties different to those described above.

Individual Cases. Energy and oscillator strengths of the conjoined coumarins additionally depend on the position and nature of the substituted group. A decrease in the transition energy and oscillator strength of this transition is observed when changing the position of the amino group from the 7- to 6-position (coumarins **3** vs **8**) and is illustrated in Figure 10.

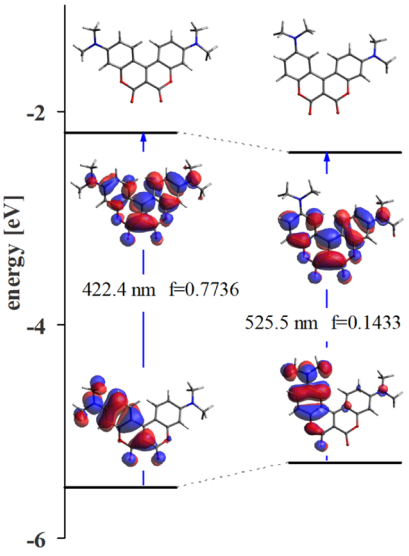

Figure 10. Influence of the position of the amino group in one of the subunits of conjoined coumarins **3** and **8** on the oscillator strength and the transition energy between states $S_0 \rightarrow S_1$ (for better comparison between both coumarins, amine in the 6-position of dye **8** was computed with two Me groups).

The HOMOs in the conjoined biscoumarins **3** and **8** are highly localized and retain the shape of the orbitals from one of the components (7-aminocoumarin or 6-aminocoumarin). In contrast, the LUMOs are delocalized over both components and are the sum of the LUMOs of each component (Figure 10). Thus, the properties of HOMO → LUMO transitions in individual components are transferred to coumarins **3** and **8**, resulting in small oscillator strength and small Φ_F in the case of dye **8**.

A change in the nature of a functional group, such as the presence of a NO_2 group (with two low-lying LUMOs), leads

https://doi.org/10.1021/acs.joc.2c00232
J. Org. Chem. 2022, 87, 5961−5975

to a more complex system of LUMO states in the coumarin core. In energetic proximity to the typical LUMO of the coumarins discussed above (i.e., LUMO delocalized across the whole molecule), a "new" LUMO appears, localized on the coumarin moieties bearing the NO_2 group (Figure 11). The

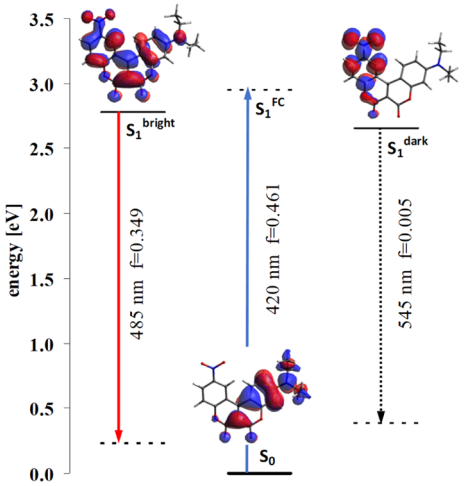

Figure 11. Diagram of electronic states for conjoined biscoumarin **7** (dark and bright forms).

absorption of conjoined coumarin **7** is analogous to the previously discussed coumarins, but in the excited state the lowest energy state becomes the one described by the "new" LUMO. This is a dark state, meaning the emission from this state is a pure CT transition with negligible oscillator strength.

Nevertheless, testing the potential energy surface in the excited state of coumarin **7** in toluene, another local energy minimum for the excited state was also found (all vibration frequencies were positive). Figure 11 summarizes the energies and oscillator strength of the electronic transitions for coumarin **7**. The energy ordering of states, $E^{FC} > E$ (bright) $> E$ (dark), shows that the energy of the bright state is lower than the excitation energy, that is, it is possible to fill it after excitation. However, the energy of the bright state is higher than the energy of the dark state.

The efficient emission of compound **7** is rare among generally nonfluorescent nitro compounds.[38] In particular, the counterpart of the compound **7**, V-shaped biscoumarin, in which the 6-nitrocoumarin moiety is replaced by 7-nitrocoumarin scaffold, is also nonfluorescent.[23] The nitrocoumarin moieties are responsible for the shape and arrangement of the low-lying LUMOs of the entire V-shaped conjoined biscoumarin. When comparing the shape of the frontier orbitals of both nitrocoumarins (as shown in Figure S9), the similar shape of their LUMOs can be seen. These LUMOs contribute to the formation of the S_1 state of the dark form of compound **7** and the S_1 state in its nonfluorescent counterpart (involving 7-nitrocoumarin). It can also be seen that the adjacent LUMO + 1 orbital, responsible for the formation of the bright form of compound **7**, is a characteristic feature only of the 6-nitrocoumarin core, absent in the case of 7-nitrocoumarin. Thus, in the differentiation of the properties of compound **7** and the regioisomeric V-shaped conjoined biscoumarin, we have an example of the wider problem of the strong differentiation of properties of coumarins with substituents in the 6 and 7 positions, which already has its own literature.[6,46]

The two V-shaped coumarins **18** and **19** differ by way of rigidification of the bridging nitrogen atom but the results of calculating the electronic structure in the ground state does not show any major differences between them. This is confirmed by the experimental absorption and emission energies. However, while Φ_F of dye **19** is large, the fluorescence of **18** is negligible. An analogous observation was made earlier for a number of coumarins with a similar structure.[24] The reason was the formation of a dark form with deformed geometry in the excited state (Figure 12). As a result of this deformation, the electronic transition becomes a pure intermolecular CT transition with practically zero oscillator strength.

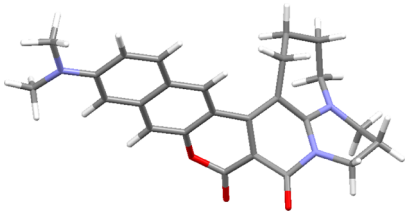

Figure 12. Deformed structure of compound **18** in the excited state [$E(S_1 \rightarrow S_0)$ = 0.9640 eV and f = 0.0009].

CONCLUSIONS

We have shown that it is possible to extend a previously developed methodology to prepare conjoined V-shaped coumarins from benzo[*g*]coumarins and benzo[*f*]coumarins. All molecules are highly polarized in the ground and excited electronic states. The HOMOs of the conjoined coumarins are localized on a single coumarin subunit (the one that exhibits the larger ionization potential). In contrast, the LUMOs are a sum of the LUMOs of both subunits and are therefore delocalized over the entire molecule. As a result of this, the direction of the dipole moment changes upon excitation. The two lowest excited electronic states S_1 and S_2, which are a result of the HOMO → LUMO and HOMO − 1 → LUMO transitions, exhibit a partial CT character as the charge transfer takes place from one of the subunits to the entire molecule. Most of the novel coumarins studied are strongly fluorescent in all solvents; however, placing one amino group at position 6, as in coumarin **8**, changes the photophysics entirely. The significant Coulomb interaction-driven stabilization originating from the larger charge separation in the S_1 excited state of this coumarin leads to lower energy of the $S_1 \rightarrow S_0$ transition and a significant drop in oscillator strength. Introducing only moderate charge transfer character into a conjoined biscoumarin possessing an NO_2 group is a viable strategy to induce strong fluorescence in nonpolar solvents. The results clearly demonstrate that unrestricted dimethyl- or diethylamino groups are better electron donors than their restricted counterpart. A similar effect is observed while comparing 7-substituted versus 6-substituted V-shaped conjoined biscoumarins. These conclusions are valid for the ground state as well as for the excited electronic state. The V-shaped biscoumarins are highly polarized and highly luminescent in contrast with previously studied amide-bridged biscoumarins of (intended) head-to-tail alignment, which, due to their flexible linker, showed a tendency to bend[37] or even curl themselves.[43] Apparently, the rigid structure of conjoined coumarin assures concurrently the high dipole moment and efficient fluorescence. Our findings demonstrate that these molecules

https://doi.org/10.1021/acs.joc.2c00232
J. Org. Chem. 2022, 87, 5961−5975

constitute a unique π-system in which large changes in the dipole moments between ground and excited states, combined with a substantial change of dipole direction, lead to appreciable photophysical properties.

EXPERIMENTAL SECTION

General Information. All reported NMR spectra (^{1}H NMR and ^{13}C NMR) were recorded using Varian 500 and 600 or Bruker 500 spectrometers. Chemical shifts (δ ppm) were determined with TMS as the internal reference, and J values are given in Hz. High-resolution mass spectra (HRMS) were obtained via an electron ionization (EI) source and a EBE double focusing geometry mass analyzer or spectrometer equipped with an electrospray ion source with a q-TOF type mass analyzer. Chromatography was performed on silica gel 60 (230−400 mesh), and thin layer chromatography (TLC) was performed on TLC plates (Merck, silica gel 60 F_{254}). Yields of conjoined biscoumarins were always calculated based on the amount of aminophenol used.

Photophysical Measurements. Room-temperature measurements were performed with dilute solutions in standard cuvettes (10 × 10 mm). Absorption spectra at room temperature (21 °C) were recorded using a PerkinElmer LAMBDA 35 spectrophotometer. Emission spectra were obtained using a FLS 1000 of Edinburgh Instruments spectrofluorometer. Fluorescence kinetics studies were performed using the time-correlated single-photon counting technique.[44] A mode-locked Coherent Mira-HP picosecond laser pumped by a Verdi 18 laser was used for excitation. The fundamental pulses of the Mira laser (tunable within 760−800 nm) were upconverted to ∼390 nm. The temporal width of the excitation pulses was ∼280 fs and of the instrument response function was about 40 ps. Fluorescence was dispersed with a 0.25 m Jarrell-Ash monochromator and detected with a HMP-100-07 hybrid detector coupled to an SPC-150 PC module (Becker&Hickl GmbH). Fluorescence decays were analyzed with deconvolution software using a nonlinear least squares procedure with the Marquardt algorithm.[45] A standard χ^2 test as well as residual and autocorrelation function plots were used to assess the quality of a fit. The estimated accuracy for the determination of decay time was below 10 ps.

Synthesis. *Synthesis of Compound 3.* A round bottom flask was charged with methyl 7-(diethylamino)-2-oxo-2*H*-chromene-3-carboxylate (**1**) (2.75 g, 10.0 mmol), 3-diethylaminophenol (**2**) (825 mg, 5.0 mmol), and $AlCl_3$ (220 mg, 1.65 mmol). The reaction mixture was stirred (neat) at 140 °C (oil bath) for 24 h. Then, the mixture was cooled to room temperature, dissolved in a small amount of DCM, and purified by column chromatography (silica, DCM/acetone 95:5) to afford a product of analytical purity.

Compound 3. Brownish precipitate. Yield: 0.142 g (7%). mp 248−250 °C. ^{1}H NMR ($CDCl_3$, 500 MHz): δ 8.01 (d, J = 9.3 Hz, 2H), 6.63 (dd, J = 9.3, 2.6 Hz, 2H), 6.47 (d, J = 2.7 Hz, 2H), 3.45 (q, J = 7.1 Hz, 8H), 1.24 (t, J = 7.1 Hz, 12H). ^{13}C{^{1}H} NMR ($CDCl_3$, 125 MHz): δ 158.0, 157.7, 152.11, 152.07, 130.1, 108.9, 104.5, 97.7, 95.9, 44.9, 12.5. HRMS (ESI) m/z: calcd for $C_{24}H_{26}N_2O_4Na$, 429.1790 [M + Na^+]; found, 429.1781.

Synthesis of Compound 5. A round bottom flask was charged with methyl 7-(diethylamino)-2-oxo-2*H*-chromene-3-carboxylate (**1**) (14.6 g, 53.0 mmol), 8-hydroxyjulolidine (**4**) (5 g, 26.95 mmol), and DMAP (323 mg, 2.65 mmol). The reaction mixture was stirred (neat) at 140 °C (oil bath) for 24 h. Then, the mixture was cooled to room temperature, dissolved in a small amount of DCM, purified by column chromatography (silica, DCM/acetone 95:5), and crystallized from *i*-PrOH-DMF to afford a product of analytical purity.

Compound 5. Orange precipitate. Yield: 10.31 g (89%). mp 205 °C (decomp). ^{1}H NMR ($CDCl_3$, 500 MHz): δ 7.95 (d, J = 9.3 Hz, 1H), 7.56 (s, 1H), 6.62 (dd, J = 9.5, 2.3 Hz, 1H), 6.45 (d, J = 2.3 Hz, 1H), 3.44 (q, J = 7.0 Hz, 4H), 3.35 (t, J = 5.5 Hz, 2H), 3.31 (t, J = 5.5 Hz, 2H), 2.87−2.77 (m, 4H), 2.01 (t, J = 5.5 Hz, 2H), 1.95 (t, J = 5.5 Hz, 2H), 1.23 (t, J = 7.0 Hz, 6H). ^{13}C{^{1}H} NMR ($CDCl_3$, 125 MHz): δ 158.3, 158.2, 157.4, 152.5, 151.9, 151.8, 147.8, 130.3, 126.0, 118.5, 108.7, 106.4, 104.6, 104.1, 97.6, 95.1, 50.1, 49.6, 44.9, 27.7, 21.3, 20.4, 20.3, 12.5. HRMS (ESI) m/z: calcd for $C_{26}H_{27}N_2O_4$, 431.1971 [M + H^+]; found, 431.1966.

Synthesis of Compound 7. A round bottom flask was charged with ethyl 6-nitro-2-oxo-2*H*-chromene-3-carboxylate (**6**) (2.1 g, 8 mmol), 3-diethylaminophenol (**2**) (660 mg, 4 mmol), and $In(OTf)_3$ (50 mg, 0.08 mmol). The reaction mixture was stirred (neat) at 140 °C (oil bath) for 5 h. Then, the mixture was cooled to room temperature. The resulting precipitate was crystalized from MeOH to afford a product of analytical purity.

Compound 7. Orange precipitate. Yield: 1.27 g (83%). mp 243−244 °C. ^{1}H NMR ($CDCl_3$, 500 MHz): δ 9.19 (d, J = 2.4 Hz, 1H), 8.51 (dd, J = 9.1, 2.5 Hz, 1H), 8.05 (d, J = 9.5 Hz, 1H), 7.54 (d, J = 9.1 Hz, 1H), 6.83 (dd, J = 9.4, 2.6 Hz, 1H), 6.59 (d, J = 2.6 Hz, 1H), 3.54 (q, J = 7.2 Hz, 4H), 1.31 (t, J = 7.2 Hz, 6H). ^{13}C{^{1}H} NMR ($CDCl_3$, 125 MHz): δ 158.5, 156.3, 155.1, 153.4, 150.4, 143.7, 129.3, 128.3, 124.8, 119.3, 116.3, 110.8, 103.6, 100.1, 98.0, 45.3, 12.5. HRMS (EI): m/z: calcd for $C_{20}H_{16}N_2O_6$, 380.1008 [$M^{\bullet+}$]; found, 380.0999.

Synthesis of Compound 8. Tin dichloride dihydrate (678 mg, 3 mmol) was added to the solution of compound **7** (285 mg, 0.75 mmol) in ethanol (50 ml). The reaction mixture was refluxed (oil bath) for 5 h. Then, the mixture was cooled to room temperature and aqueous $NaHCO_3$ was added until the pH became neutral. The aqueous solution was extracted with DCM, and the combined organic layers were dried over Na_2SO_4 and concentrated under reduced pressure. The crude product was purified by column chromatography (silica, DCM/acetone 4:1) and crystallized from DCM-Et_2O affording a product of analytical purity.

Compound 8. Red precipitate. Yield: 0.142 g (54%). mp 133−135 °C. ^{1}H NMR (CD_3CN, 500 MHz): δ 8.19 (d, J = 9.4 Hz, 1H), 7.50 (d, J = 2.5 Hz, 1H), 7.14 (d, J = 8.8 Hz, 1H), 7.04 (dd, J = 8.8, 2.6 Hz, 1H), 6.77 (dd, J = 9.4, 2.7 Hz, 1H), 6.56 (d, J = 2.7 Hz, 1H), 4.35 (br s, 2H), 3.51 (q, J = 7.1 Hz, 4H), 1.21 (t, J = 7.1 Hz, 6H). ^{13}C{^{1}H} NMR ($CDCl_3$, 125 MHz): δ 157.9, 157.4, 157.3, 152.6, 152.1, 147.9, 143.1, 130.1, 122.2, 118.6, 116.3, 112.4, 109.6, 104.2, 100.3, 97.5, 45.1, 12.5. HRMS (EI): m/z: calcd for $C_{20}H_{18}N_2O_4$, 350.1267 [$M^{\bullet+}$]; found, 350.1280.

General Procedure for the Synthesis of Compounds 10−13. A round bottom flask was charged with ethyl 8-(dimethylamino)-2-oxo-2*H*-benzo[*g*]chromene-3-carboxylate (**9**) (156 mg, 0.5 mmol), appropriate phenol (3-diethylaminophenol (**2**) (41 mg, 0.25 mmol), 8-hydroxyjulolidine (**4**) (47 mg, 0.25 mmol), 3-ethylamino-*p*-cresol (38 mg, 0.25 mmol) or 7-hydroxy-1,2,3,4-tetrahydroquinoline (37 mg, 0.25 mmol)), and DMAP (0.6 mg, 0.005 mmol). The reaction mixture was stirred (neat) at 140 °C (oil bath) for 5 h. Then the mixture was cooled to room temperature, dissolved in a small amount of DCM, and purified by column chromatography (silica, DCM/MeOH 98:2). Crystallization from MeOH afforded a product of analytical purity.

Compound 10. Brown precipitate. Yield: 0.036 g (34%). mp 250 °C (decomp). ^{1}H NMR (CD_2Cl_2, 500 MHz): δ 8.51 (s, 1H), 8.16 (d, J = 9.4 Hz, 1H), 7.80 (d, J = 9.2 Hz, 1H), 7.37 (s, 1H), 7.15 (dd, J = 9.2, 2.5 Hz, 1H), 6.78−6.73 (m, 2H), 6.53 (d, J = 2.7 Hz, 1H), 3.51 (q, J = 7.1 Hz, 4H), 3.13 (s, 6H), 1.28 (t, J = 7.1 Hz, 6H). ^{13}C{^{1}H} NMR (CD_2Cl_2, 125 MHz): δ 158.5, 157.5, 157.4, 153.05, 153.03, 151.9, 151.3, 138.5, 131.0, 130.9, 130.8, 123.6, 116.4, 112.3, 110.4, 110.0, 104.9, 103.4, 98.9, 97.9, 45.4, 40.4, 12.7. HRMS (EI): m/z: calcd for $C_{26}H_{24}N_2O_4$, 428.1736 [$M^{\bullet+}$]; found, 428.1748.

Compound 11. Red precipitate. Yield: 0.044 g (39%). mp 230 °C (decomp). ^{1}H NMR (CD_2Cl_2, 500 MHz): δ 8.54 (s, 1H), 7.83 (d, J = 9.2 Hz, 1H), 7.78 (s, 1H), 7.43 (s, 1H), 7.18 (d, J = 9.3 Hz, 1H), 6.83 (s, 1H), 3.42−3.36 (m, 4H), 3.15 (s, 6H), 2.92−2.84 (m, 4H), 2.07−1.99 (m, 4H). ^{13}C{^{1}H} NMR (CD_2Cl_2, 125 MHz): δ 155.54, 155.47, 153.87, 153.47, 153.44, 151.4, 140.6, 133.5, 133.3, 128.9, 125.8, 122.4, 118.6, 114.7, 112.6, 110.0, 109.0, 106.9, 52.8, 52.3, 42.6, 30.4, 23.8, 22.8. HRMS (EI): m/z: calcd for $C_{28}H_{24}N_2O_4$: 452.1736 [$M^{\bullet+}$]; found, 452.1729.

Compound 12. Dark red precipitate. Yield: 0.037 g (36%). mp 296 °C (decomp). ^{1}H NMR (CD_2Cl_2, 500 MHz): δ 8.58 (s, 1H), 8.02 (s, 1H), 7.85 (d, J = 9.2 Hz, 1H), 7.44 (s, 1H), 7.20 (dd, J = 9.2, 2.3 Hz,

https://doi.org/10.1021/acs.joc.2c00232
J. Org. Chem. 2022, 87, 5961−5975

1H), 6.86 (s, 1H), 6.52 (s, 1H), 4.51 (br s, 1H), 3.36 (q, J = 7.2 Hz, 2H), 3.15 (s, 6H), 2.27 (s, 3H), 1.38 (t, J = 7.2 Hz, 3H). $^{13}C\{^1H\}$ NMR (CD_2Cl_2, 125 MHz): δ 157.2, 157.1, 157.0, 152.9, 152.2, 151.4, 150.7, 138.0, 130.7, 130.6, 129.2, 123.2, 119.6, 116.0, 112.1, 110.1, 105.0, 103.4, 99.3, 96.0, 40.2, 38.3, 17.1, 14.1. HRMS (EI): m/z: calcd for $C_{25}H_{22}N_2O_4$, 414.1580 [$M^{\bullet+}$]; found, 414.1582.

Compound 13. Brown precipitate. Yield: 0.042 g (41%). mp 248 °C (decomp). ^1H NMR (DMSO-d_6, 500 MHz): δ 8.72 (s, 1H), 8.06 (d, J = 9.3 Hz, 1H), 7.94 (s, 1H), 7.68 (br s, 1H), 7.47 (s, 1H), 7.27 (dd, J = 9.3, 2.5 Hz, 1H), 6.91 (d, J = 2.1 Hz, 1H), 6.38 (s, 1H), 3.38−3.32 (m, 2H, overlap by signal from DMSO), 3.12 (s, 6H), 2.87 (t, J = 5.9 Hz, 2H), 1.91−1.83 (m, 2H). $^{13}C\{^1H\}$ NMR (DMSO-d_6, 125 MHz): δ 156.4, 156.2, 155.9, 152.0, 151.9, 150.8, 150.7, 137.6, 131.3, 130.9, 129.3, 122.8, 119.2, 115.9, 111.2, 109.3, 103.7, 102.7, 97.5, 96.6, 40.5 (overlap by signal from DMSO), 40.1 (overlap by signal from DMSO), 26.3, 20.5. HRMS (ESI) m/z: calcd for $C_{25}H_{20}N_2O_4Na$, 435.1321 [M + Na^+]; found, 435.1322.

*General Procedure for the Synthesis of Compounds **15**−**17**.* A round bottom flask was charged with ethyl 3-oxo-3*H*-benzo[*f*]-chromene-2-carboxylate (**14**) (402 mg, 1.5 mmol), appropriate phenol (8-hydroxyjulolidine (**4**) (142 mg, 0.75 mmol), 3-ethylamino-*p*-cresol (113 mg, 0.75 mmol) or 7-hydroxy-1,2,3,4-tetrahydroquinoline (112 mg, 0.75 mmol)), and DMAP (2 mg, 0.015 mmol). The reaction mixture was stirred (neat) at 140 °C (oil bath) for 5 h. The mixture was then cooled to room temperature, dissolved in a small amount of DCM, and purified by column chromatography (silica, DCM/acetone 9:1). Crystallization from MeOH afforded a product of analytical purity.

Compound 15. Red precipitate. Yield: 0.096 g (31%). mp 159 °C (decomp). ^1H NMR ($CDCl_3$, 600 MHz): δ 8.13 (d, J = 8.6 Hz, 1H), 8.04 (d, J = 8.9 Hz, 1H), 7.87 (d, J = 7.9 Hz, 1H), 7.49 (ddd, J = 8.0, 6.9, 1.0 Hz, 1H), 7.44 (d, J = 8.9 Hz, 1H), 7.38 (ddd, J = 8.3, 6.9, 1.3 Hz, 1H), 7.10 (s, 1H), 3.42−3.32 (m, 4H), 3.02−2.90 (m, 2H), 2.60−2.54 (m, 1H), 2.50−2.44 (m, 1H), 2.11−1.83 (m, 4H). $^{13}C\{^1H\}$ NMR ($CDCl_3$, 125 MHz): δ 157.6, 157.3, 154.7, 153.1, 152.8, 148.8, 135.1, 131.0, 129.9, 128.5, 127.6, 126.7, 126.1, 125.8, 117.8, 117.3, 110.6, 106.1, 105.1, 99.7, 50.2, 49.9, 27.3, 21.2, 20.31, 20.27. HRMS (EI): m/z: calcd for $C_{26}H_{19}NO_4$, 409.1314 [$M^{\bullet+}$]; found, 409.1319.

Compound 16. Yellow precipitate. Yield: 0.049 g (18%). mp 304 °C (decomp). ^1H NMR (DMSO-d_6, 500 MHz): δ 8.29 (d, J = 9.0 Hz, 1H), 8.04 (d, J = 7.9 Hz, 1H), 8.02 (d, J = 8.7 Hz, 1H), 7.58−7.52 (m, 2H), 7.47 (ddd, J = 8.4, 7.0, 1.3 Hz, 1H), 7.14 (s, 1H), 6.71 (t, J = 5.5 Hz, 1H), 6.51 (s, 1H), 3.31 (q, J = 7.1 Hz, 2H, overlap by signal from DMSO), 1.89 (s, 3H), 1.22 (t, J = 7.1 Hz, 3H). $^{13}C\{^1H\}$ NMR (DMSO-d_6, 125 MHz): δ 157.3, 156.7, 156.4, 154.6, 153.8, 153.2, 136.2, 131.1, 130.5, 129.7, 129.1, 126.9, 126.8, 126.4, 119.4, 117.3, 110.3, 104.8, 99.9, 94.9, 37.9, 17.6, 14.4. HRMS (EI): m/z: calcd for $C_{23}H_{17}NO_4$, 371.1158 [$M^{\bullet+}$]; found, 371.1154.

Compound 17. Orange precipitate. Yield: 0.051 g (18%). mp 280 °C (decomp). ^1H NMR ($CDCl_3$, 600 MHz): δ 8.15 (d, J = 8.4 Hz, 1H), 8.07 (d, J = 8.9 Hz, 1H), 7.90 (d, J = 8.0 Hz, 1H), 7.52 (ddd, J = 7.9, 7.1, 0.8 Hz, 1H), 7.46 (d, J = 8.9 Hz, 1H), 7.43 (ddd, J = 8.4, 7.2, 1.1 Hz, 1H), 7.28 (s, 1H), 6.51 (s, 1H), 5.39 (s, 1H), 3.48−3.44 (m, 2H), 2.65−2.59 (m, 1H), 2.53−2.47 (m, 1H), 2.02−1.94 (m, 1H), 1.90−183 (m, 1H). $^{13}C\{^1H\}$ NMR ($CDCl_3$, 125 MHz): δ 157.5, 157.1, 156.3, 154.9, 153.6, 151.7, 135.5, 131.0, 130.5, 129.8, 128.6, 126.6, 126.3, 126.0, 118.0, 117.3, 110.4, 105.9, 100.8, 98.6, 41.7, 26.5, 21.0. HRMS (EI): m/z: calcd for $C_{23}H_{15}NO_4$, 369.1001 [$M^{\bullet+}$]; found, 369.1007.

*General Procedure for the Synthesis of Compounds **18** and **19**.* A round bottom flask was charged with ethyl 8-(dimethylamino)-2-oxo-2*H*-benzo[*g*]chromene-3-carboxylate (**9**) (415 mg, 1.5 mmol) and DBU (225 μL, 0.75 mmol) or DBN (93 μL, 0.75 mmol). The reaction mixture was stirred (neat) at 120 °C (oil bath) in an open flask for 2 h in the case of DBU or 30 min in the case of DBN. Then, the mixture was cooled to room temperature. The resulting precipitate was crystalized from EtOH to afford a product of analytical purity.

Compound 18. Yellow precipitate. Yield: 0.185 g (59%). mp 250 °C (decomp). ^1H NMR ($CDCl_3$, 500 MHz): δ 8.19 (s, 1H), 7.66 (d, J = 9.0 Hz, 1H), 7.35 (s, 1H), 7.06 (d, J = 9.0 Hz, 1H), 6.75 (s, 1H), 4.21 (br s, 2H), 3.71 (br s, 2H), 3.40 (t, J = 6.3 Hz, 2H), 3.10 (s, 8H), 2.13−2.00 (m, 4H), 1.97−1.89 (m, 2H). $^{13}C\{^1H\}$ NMR ($CDCl_3$, 125 MHz): δ 158.9, 158.5, 155.0, 151.2, 151.1, 150.0, 136.8, 129.9, 129.7, 122.5, 115.4, 114.5, 110.1, 103.7, 98.0, 97.9, 53.4, 49.3, 40.4, 38.8, 31.6, 25.0, 24.9, 22.8. HRMS (ESI) m/z: calcd for $C_{25}H_{25}N_3O_3Na$, 438.1794 [M + Na^+]; found, 438.1788.

Compound 19. Yellow precipitate. Yield: 0.212 g (73%). mp 310 °C (decomp). ^1H NMR (CD_2Cl_2, 500 MHz): δ 7.84 (s, 1H), 7.49 (d, J = 9.4 Hz, 1H), 7.21 (s, 1H), 6.97 (dd, J = 9.0, 1.9 Hz, 1H), 6.67 (d, J = 2.0 Hz, 1H), 3.89−3.80 (m, 4H), 3.37−3.33 (m, 2H), 3.32−3.25 (m, 2H), 3.08 (s, 6H), 2.18−2.09 (m, 2H). $^{13}C\{^1H\}$ NMR (CD_2Cl_2, 125 MHz): δ 159.6, 155.5, 150.8, 149.9, 141.6, 136.5, 129.7, 127.3, 122.8, 115.2, 113.9, 110.0, 109.4, 103.1, 96.5, 90.1, 51.6, 42.0, 40.1, 37.5, 27.4, 19.5. HRMS (EI): m/z: calcd for $C_{23}H_{21}N_3O_3$, 387.1583 [$M^{\bullet+}$]; found, 387.1592.

*Synthesis of Compound **20**.* A round bottom flask was charged with ethyl 3-oxo-3*H*-benzo[*f*]chromene-2-carboxylate (**14**) (402 mg, 1.5 mmol) and DBN (93 μL, 0.75 mmol). The reaction mixture was stirred (neat) at 120 °C (oil bath) in an open flask for 30 min. The mixture was then cooled to room temperature, dissolved in a small amount of DCM, and purified by column chromatography (silica, DCM/MeOH 95:5). Crystallization from MeOH afforded a product of analytical purity.

Compound 20. Yellow precipitate. Yield: 0.097 g (38%). mp 196−198 °C. ^1H NMR ($CDCl_3$, 500 MHz): δ 7.89−7.84 (m, 2H), 7.66 (d, J = 8.3 Hz, 1H), 7.51 (ddd, J = 8.2, 7.0, 1.3 Hz, 1H), 7.45 (ddd, J = 8.0, 6.9, 1.1 Hz, 1H), 7.27 (d, J = 7.9 Hz, 1H), 4.08 (t, J = 5.9 Hz, 2H), 3.75 (br s, 2H), 3.43 (t, J = 5.6 Hz, 2H), 2.23 (quintet, J = 5.9 Hz, 2H), 1.69 (s, 2H). $^{13}C\{^1H\}$ NMR ($CDCl_3$, 125 MHz): δ 159.22, 159.18, 156.5, 153.3, 143.8, 132.9, 130.7, 128.6, 128.57, 126.6, 126.1, 124.9, 117.4, 111.5, 98.1, 93.3, 52.1, 42.6, 38.0, 28.7, 20.1. HRMS (ESI) m/z: calcd for $C_{21}H_{16}N_2O_3Na$, 367.1059 [M + Na^+]; found, 367.1059.

*Formation of Spiro-coumarin **21**.* Compound **19** (120 mg, 0.31 mmol) was dissolved in DCM (500 ml) and the reaction mixture was exposed to the air and sunlight for 2 weeks. After this time, the solvent was evaporated and the crude product was purified by column chromatography (silica, DCM/MeOH 95:5) and crystallized from MeOH affording a product of analytical purity.

*Spiro-coumarin **21**.* Red precipitate. Yield: 0.023 g (18%). mp 235 °C (decomp). ^1H NMR ($CDCl_3$, 500 MHz): δ 7.74 (d, J = 9.2 Hz, 1H), 7.68 (s, 1H), 7.48 (s, 1H), 7.14 (dd, J = 9.2, 2.4 Hz, 1H), 6.79 (d, J = 2.5 Hz, 1H), 3.82−3.75 (m, 1H), 3.65 (t, J = 8.6 Hz, 1H), 3.54−3.50 (m, 1H), 3.46−3.39 (m, 2H), 3.36−3.28 (m, 1H), 3.17 (s, 6H), 2.88−2.79 (m, 1H), 2.53−2.46 (m, 1H), 1.92−1.86 (m, 2H). $^{13}C\{^1H\}$ NMR (CD_2Cl_2, 150 MHz): δ 168.1, 165.2, 156.8, 155.0, 152.6, 151.2, 139.2, 130.7, 126.4, 123.1, 116.5, 110.5, 109.4, 109.2, 103.5, 87.9, 48.7 (overlap by signal from MeOH), 43.7, 43.6, 40.0, 33.4, 19.8. HRMS (EI): m/z: calcd for $C_{23}H_{21}N_3O_4$, 403.1532 [$M^{\bullet+}$]; found, 403.1518.

■ ASSOCIATED CONTENT

Supporting Information

The Supporting Information is available free of charge at https://pubs.acs.org/doi/10.1021/acs.joc.2c00232.

Synthesis details, X-ray crystallographic information; photophysical data; theoretical data; copies of ^1H and $^{13}C\{^1H\}$ NMR spectra; and X-ray crystal data for **21** (PDF)

Cartesian coordinates related to computational studies (PDF)

Accession Codes

CCDC 2144352 contains the supplementary crystallographic data for this paper. These data can be obtained free of charge

https://doi.org/10.1021/acs.joc.2c00232
J. Org. Chem. 2022, 87, 5961−5975

via www.ccdc.cam.ac.uk/data_request/cif, or by emailing data_request@ccdc.cam.ac.uk, or by contacting The Cambridge Crystallographic Data Centre, 12 Union Road, Cambridge CB2 1EZ, UK; fax: +44 1223 336033.

AUTHOR INFORMATION

Corresponding Authors

Irena Deperasińska − *Institute of Physics of Polish Academy of Sciences, 02-668 Warsaw, Poland*; Email: deper@ifpan.edu.pl

Daniel T. Gryko − *Institute of Organic Chemistry of Polish Academy of Sciences, 01-224 Warsaw, Poland*; orcid.org/0000-0002-2146-1282; Email: dtgryko@icho.edu.pl

Authors

Łukasz Kielesiński − *Institute of Organic Chemistry of Polish Academy of Sciences, 01-224 Warsaw, Poland*

Olaf Morawski − *Institute of Physics of Polish Academy of Sciences, 02-668 Warsaw, Poland*

Kateryna V. Vygranenko − *Institute of Organic Chemistry of Polish Academy of Sciences, 01-224 Warsaw, Poland*

Erik T. Ouellette − *Department of Chemistry, University of California, Berkeley, Berkeley, California 94720, United States; Chemical Sciences Division, Lawrence Berkeley National Laboratory, Berkeley, California 94720, United States*; orcid.org/0000-0003-2138-6259

Complete contact information is available at: https://pubs.acs.org/10.1021/acs.joc.2c00232

Author Contributions

This manuscript was written through contributions of all authors. All authors have given approval to the final version of the manuscript.

Notes

The authors declare no competing financial interest.

ACKNOWLEDGMENTS

This work was financially supported by the Polish National Science Center, Poland (OPUS 2020/37/B/ST4/00017, the QuantERA programme—project 2017/25/Z/ST2/03038, and the Foundation for Polish Science (TEAM POIR.04.04.00-00-3CF4/16-00). This project received funding from the EU's Horizon 2020 research and innovation programme under grant agreement no 860762 (MSC ITN CHAIR). The Advanced Light Source (ALS) is supported by the Director, Office of Science, Office of Basic Energy Sciences, of the U.S. DOE under contract no. DE-AC02-05CH11231. Dr. Simon J. Teat is thanked for his assistance during crystallography experiments at the ALS. We thank Dr. David C. Young for amending the manuscript. This research was carried out with the support of the Interdisciplinary Centre for Mathematical and Computational Modelling ICM University of Warsaw under computational allocation no G87-1090.

REFERENCES

(1) von Pechmann, H., II; Welsh, W. Ueber Einige Neue Cumarine. *Ber. Dtsch. Chem. Ges.* **1884**, *17*, 1646−1652.

(2) (a) Soine, T. O. Naturally Occurring Coumarins and Related Physiological Activities. *J. Pharm. Sci.* **1964**, *53*, 231−264. (b) Kowalik, L.; Chen, J. K. Illuminating Developmental Biology Through Photochemistry. *Nat. Chem. Biol.* **2017**, *13*, 587−598. (c) Nadler, A.; Yushchenko, D. A.; Müller, R.; Stein, F.; Feng, S.; Mulle, C.; Carta, M.; Schultz, C. Exclusive Photorelease of Signalling Lipids at the Plasma Membrane. *Nat. Commun.* **2015**, *6*, 10056.

(3) Sardari, S.; Mori, Y.; Horita, K.; Micetich, R. G.; Nishibe, S.; Daneshtalab, M. Synthesis and Antifungal Activity of Coumarins and Angular Furanocoumarins. *Bioorg. Med. Chem.* **1999**, *7*, 1933−1940.

(4) García-Argáez, A.; Ramírez Apan, T.; Delgado, H.; Velázquez, G.; Martínez-Vázquez, M. Anti-Inflammatory Activity of Coumarins from Decatropis Bicolor on TPA Ear Mice Model. *Planta Med.* **2000**, *66*, 279−281.

(5) (a) Schiedel, M.-S.; Briehn, C. A.; Bäuerle, P. Single-Compound Libraries of Organic Materials: Parallel Synthesis and Screening of Fluorescent Dyes. *Angew. Chem., Int. Ed.* **2001**, *40*, 4677−4680. (b) Wang, D.; Ma, Z.; Wang, N.; Li, C.; Wang, T.; Liang, Y.; Zhang, Z. Synthesis of 7-Hydroxy-6H-Naphtho[2,3-c]Coumarin via TsOH-Mediated tandem Reaction. *Chem. Commun.* **2020**, *56*, 10369−10372. (c) Xue, W.; Wang, D.; Li, C.; Zhai, Z.; Wang, T.; Liang, Y.; Zhang, Z. π-Expanded Coumarins: One-Pot Photo Synthesis of 5H-Benzo-[12,1]Tetrapheno[7,6,5-cde)Chromen-5-Ones and Photophysical properties. *J. Org. Chem.* **2020**, *85*, 3689−3698. (d) Li, C.; Wang, D.; Xue, W.; Peng, J.; Wang, T.; Zhang, Z. Synthesis and Photophysical Properties of Vertically π-Expanded Coumarins. *Dyes Pigm.* **2021**, *186*, 108956.

(6) (a) Xie, L.; Chen, Y.; Wu, W.; Guo, H.; Zhao, J.; Yu, X. Fluorescent Coumarin Derivatives with Large Stokes Shift, Dual Emission and Solid State Luminescent Properties: An Experimental and Theoretical Study. *Dyes Pigm.* **2012**, *92*, 1361−1369. (b) Krystkowiak, E.; Dobek, K.; Burdziński, G.; Maciejewski, A. Radiationless Deactivation of 6-Aminocoumarin From the S_1-ICT State in Nonspecifically Interacting Solvents. *Photochem. Photobiol. Sci.* **2012**, *11*, 1322−1330. (c) Liu, X.; Cole, J. M.; Xu, Z. Substantial Intramolecular Charge Transfer Induces Long Emission Wavelengths and Mega Stokes Shifts in 6-Aminocoumarins. *J. Phys. Chem. C* **2017**, *121*, 13274−13279.

(7) (a) Sun, X.-Y.; Liu, T.; Sun, J.; Wang, X.-J. Synthesis and Application of Coumarin Fluorescence Probes. *RSC Adv.* **2020**, *10*, 10826−10847. (b) Cao, D.; Liu, Z.; Verwilst, P.; Koo, S.; Jangjili, P.; Kim, J. S.; Lin, W. Coumarin-Based Small-Molecule Fluorescent Chemosensors. *Chem. Rev.* **2019**, *119*, 10403−10519.

(8) Mishra, A.; Fischer, M. K. R.; Bäuerle, P. Metal-Free Organic Dyes for Dye-Sensitized Solar Cells: From Structure: Property Relationships to Design Rules. *Angew. Chem., Int. Ed.* **2009**, *48*, 2474−2499.

(9) (a) Zhang, H.; Yu, T.; Zhao, Y.; Fan, D.; Xia, Y.; Zhang, P. Synthesis, Crystal Structure, Photo- and Electro-Luminescence of 3-(4-(Anthracen-10-yl)Phenyl)-7-(N,N,'-Diethylamino)Coumarin. *Synth. Met.* **2010**, *160*, 1642−1647. (b) Yan, L.; Li, R.; Shen, W.; Qi, Z. Multiple-Color AIE Coumarin-Based Schiff Bases and Potential Application in Yellow OLEDs. *J. Lumin.* **2018**, *194*, 151−155. (c) Yu, T.; Zhang, P.; Zhao, Y.; Zhang, H.; Meng, J.; Fan, D. Synthesis, Characterization and High-Efficiency Blue Electroluminescence Based on Coumarin Derivatives of 7-Diethylamino-Coumarin-3-Carboxamide. *Org. Electron.* **2009**, *10*, 653−660.

(10) (a) Raikar, U. S.; Tangod, V. B.; Mannopantar, S. R.; Mastiholi, B. M. Ground and Excited State Dipole Moments of Coumarin 337 Laser Dye. *Opt. Commun.* **2010**, *283*, 4289−4292. (b) Mannekutla, J. R.; Mulimani, B. G.; Inamdar, S. R. Solvent Effect on Absorption and Fluorescence Spectra of Coumarin Laser Dyes: Evaluation of Ground and Excited State Dipole Moments. *Spectrochim. Acta, Part A* **2008**, *69*, 419−426.

(11) (a) Niu, G.; Liu, W.; Xiao, H.; Zhang, H.; Chen, J.; Dai, Q.; Ge, J.; Wu, J.; Wang, P. Keto-Benzo[h]-Coumarin-Based Near-Infrared Dyes with Large Stokes Shifts for Bioimaging Applications. *Chem.—Asian J.* **2016**, *11*, 498−504. (b) Jung, Y.; Jung, J.; Huh, Y.; Kim, D. Benzo[g]coumarin-Based Fluorescent Probes for Bioimaging Applications. *J. Anal. Methods Chem.* **2018**, 5249765. (c) Sednev, M. V.; Belov, V. N.; Hell, S. W. Fluorescent Dyes with Large Stokes Shifts for Super-Resolution Optical Microscopy of Biological Objects: a Review. *Methods Appl. Fluoresc.* **2015**, *3*, 042004.

(12) (a) Kim, D.; Singha, S.; Wang, T.; Seo, E.; Lee, J. H.; Lee, S.-J.; Kim, K. H.; Ahn, K. H. In Vivo Two-Photon Fluorescent Imaging of Fluoride with a Desilylation-Based Reactive Probe. *Chem. Commun.* **2012**, *48*, 10243−10245. (b) Jun, Y. W.; Kim, H. R.; Reo, Y. J.; Dai, M.; Ahn, K. H. Addressing the Autofluorescence Issue in Deep Tissue Imaging by Two-Photon Microscopy: the Significance of Far-Red Emitting Dyes. *Chem. Sci.* **2017**, *8*, 7696−7704. (c) Sarkar, S.; Santra, M.; Singha, S.; Jun, Y. W.; Reo, Y. J.; Kim, H. R.; Ahn, K. H. Two-Photon absorbing 8-Hydroxybenzo[g]coumarins with Giant Stokes Shifts: an Environment-Insensitive Dye Platform for Probing Biomolecules. *J. Mater. Chem. B* **2018**, *6*, 4446−4452. (d) Hao, X.-L.; Guo, Z.-J.; Zhang, C.; Ren, A.-M. Excellent Benzocoumarin-Based Ratiometric Two-Photon Fluorescent Probe for H_2O_2 Detection. *Phys. Chem. Chem. Phys.* **2019**, *21*, 281−291.

(13) Węcławski, M. K.; Deperasińska, I.; Banasiewicz, M.; Young, D. C.; Leniak, A.; Gryko, D. T. Building Molecular Complexity from Quinizarin: Conjoined Coumarins and Coronene Analogs. *Chem.—Asian J.* **2019**, *14*, 1763−1779.

(14) (a) Mukhopadhyay, A.; Hossen, T.; Ghosh, I.; Koner, A. L.; Nau, W. M.; Sahu, K.; Moorthy, J. N. Helicity-Dependent Regiodifferentiation in the Excited-State Quenching and Chiroptical Properties of Inward/Outward Helical Coumarins. *Chem.—Eur. J.* **2017**, *23*, 14797−14805. (b) Usui, K.; Yamamoto, K.; Ueno, Y.; Igawa, K.; Hagihara, R.; Masuda, T.; Ojida, A.; Karasawa, S.; Tomooka, K.; Hirai, G.; Suemune, H. Internal-Edge-Substituted Coumarin-Fused [6]Helicenes: Asymmetric Synthesis, Structural Features, and Control of Self-Assembly. *Chem.—Eur. J.* **2018**, *24*, 14617−14621. (c) Moorthy, J. N.; Mandal, S.; Mukhopadhyay, A.; Samanta, S. Helicity as a Steric Force: Stabilization and Helicity-Dependent Reversion of Colored o-Quinonoid Intermediates of Helical Chromenes. *J. Am. Chem. Soc.* **2013**, *135*, 6872−6884. (d) Nitisha; Chetti, P.; Parthasarathy, V. Coronene-Embedded 'Super' Coumarins. *Chem. Commun.* **2022**, *58*, 431−434. (e) Sarmah, M.; Chutia, K.; Dutta, D.; Gogoi, P. Overview of Coumarin-Fused-Coumarins: Synthesis, Photophysical Properties and Their Applications. *Org. Biomol. Chem.* **2022**, *20*, 55−72. (f) Ueda, M.; Kokubun, M.; Mazaki, Y. Triskelion-Shaped π-Luminophores Bearing Coumarin: Synthesis, Structures and Luminescence Properties. *ChemPhotoChem* **2020**, *4*, 5159−5167. (g) Kumar, P.; Venkatakrishnan, P. Expanding the Family of Fluorescent Coumarin[4]arenes: Improved Synthesis, π-Extension and Characterization. *Eur. J. Org. Chem.* **2019**, 7787−7799. (h) Nitisha; Venkatakrishnan, P. Accessing [g]-Face π-Expanded Fluorescent Coumarins by Scholl Cyclization. *J. Org. Chem.* **2019**, *84*, 10679−10689. (i) Kumar, A.; Rajpoot, A.; Imroze, F.; Maddala, S.; Dutta, S.; Venkatakrishnan, P. Linear Coumarinacenes Beyond Benzo[g]coumarins: Synthesis and Promising Characteristics. *Eur. J. Org. Chem.* **2020**, 6976−6980. (j) Mukhopadhyay, A.; Jana, K.; Hossen, T.; Sahu, K.; Moorthy, J. N. Coumarin-Annelated Regioisomeric Heptahelicenes: Influence of Helicity on Excited-State Properties and Chiroptical Properties. *J. Org. Chem.* **2019**, *84*, 10658−10668.

(15) Högberg, T.; Vora, M.; Drake, S. D.; Mitscher, L. A.; Chu, D. T. W. Structure-Activity Relationships among DNA-Gyrase Inhibitors. Sytntthesis and Antimicrobial Evaluation of Chromones and Coumarins Related to Oxolinic Acid. *Acta Chem. Scand., Ser. B* **1984**, *38b*, 359−366.

(16) Poronik, E. M.; Shandura, M. P.; Kovtun, Y. P. Synthesis of 6H,7H-[1]benzopyrano[3,4-c][1]benzopyran-6,7-diones. *Chem. Heterocycl. Compd.* **2006**, *42*, 410−411.

(17) Seijas, J. A.; Crecente-Campo, J.; Vázquez-Tato, M. P. Microwave Assisted Synthesis of Coumarocoumarins. *16th International Electronic Conference on Synthetic Organic Chemistry*, 2012.

(18) (a) Xi, G.-L.; Liu, Z.-Q. Coumarin-Fused Coumarin: Antioxidant Story from N,N-Dimethylamino and Hydroxyl Groups. *J. Agric. Food Chem.* **2015**, *63*, 3516−3523. (b) Fang, Q.; Yue, X.; Han, S.; Wang, B.; Song, X. A Rapid and Sensitive Fluorescent Probe for Detecting Hydrogen Polysulfides in Living Cells and Zebra Fish. *Spectrochim. Acta, Part A* **2020**, *224*, 117410. (c) Yu, B.; Chen, C.; Ru, J.; Luo, W.; Liu, W. A Multifunctional Two-Photon Fluorescent Probe for Detecting H_2S in Wastewater and GSH in vivo. *Talanta* **2018**, *188*, 370−377.

(19) Chen, C.; Zhou, L.; Liu, F.; Li, Z.; Liu, W.; Liu, W. V-Shaped Bis-Coumarin Based Fluorescent Probe for Detecting Palladium in Natural Waters. *J. Hazard. Mater.* **2020**, *386*, 121943.

(20) Jiang, Y.; Li, H.; Chen, R.; Liu, W.; Chen, C.; Li, Z.; Liu, W. Novel Fluorescent Probe Based on Dicoumarin for Rapid On-Site Detection of Hg^{2+} in Loess. *Spectrochim. Acta, Part A* **2021**, *251*, 119438.

(21) (a) Jiang, X.; Shangguan, M.; Lu, Z.; Yi, S.; Zeng, X.; Zhang, Y.; Hou, L. A "Turn-on" Fluorescent Probe Based on V-Shaped Bis-Coumarin for Detection of Hydrazine. *Tetrahedron* **2020**, *76*, 130921. (b) Fang, Q.; Yang, L.; Xiong, H.; Han, S.; Zhang, Y.; Wang, J.; Chen, W.; Song, X. Coumarinocoumarin-Based Fluorescent Probe for the Sensitive and Selective Detection of Hydrazine in Living Cells and Zebra Fish. *Chin. Chem. Lett.* **2020**, *31*, 129−132.

(22) (a) Chen, C.; Zhou, L.; Liu, W.; Liu, W. Coumarinocoumarin-Based Two-Photon Fluorescent Cysteine Biosensor for Targeting Lysosome. *Anal. Chem.* **2018**, *90*, 6138−6143. (b) Chen, C.; Zhou, L.; Huang, X.; Liu, W. Rapid Detection of Intracellular Cys Over Hcy and GSH Using a Novel Two-Photon Coumarinocoumarin-Based Colorimetric and Fluorescent Probe. *J. Mater. Chem. B* **2017**, *5*, 5892−5897.

(23) Tasior, M.; Poronik, Y. M.; Vakuliuk, O.; Sadowski, B.; Karczewski, M.; Gryko, D. T. V-Shaped Bis-Coumarins: Synthesis and Optical Properties. *J. Org. Chem.* **2014**, *79*, 8723−8732.

(24) Poronik, Y. M.; Gryko, D. T. Pentacyclic Coumarin-Based Blue Emitters − the Case of Bifunctional Nucleophilic Behavior of Amidines. *Chem. Commun.* **2014**, *50*, 5688−5690.

(25) Lippert, E.; Lüder, W.; Moll, F.; Nägele, W.; Boos, H.; Prigge, H.; Seibold-Blankenstein, I. Umwandlung von Elektronenanregungsenergie. *Angew. Chem.* **1961**, *73*, 695−706.

(26) Rotkiewicz, K.; Grellmann, K. H.; Grabowski, Z. R. Rinterpretation of the Anomalous Fluorescence of p-N,N-Dimethylaminobenzonitrile. *Chem. Phys. Lett.* **1973**, *19*, 315−318.

(27) Haberhauer, G. Planarized and Twisted Intramolecular Charge Transfer: A Concept for Fluorophores Showing Two Independent rotations in Excited State. *Chem.—Eur. J.* **2017**, *23*, 9288−9296.

(28) (a) Lakowicz, J. R. *Principles of Fluorescence Spectroscopy*; Springer: Heidelberg, 2006; p 213. (b) Valeur, B.; Berberan-Santos, M. N. *Molecular Fluorescence Principles and Applications*, 2nd ed.; Wiley-VCH Verlag & Co. KGaA, 2012; pp 380−384.

(29) (a) Zachariasse, K. A.; Grobys, M.; Von der Haar, T.; Hebecker, A.; Il'ichev, Y. V.; Jiang, Y.-B.; Morawski, O.; Kühnle, W. Intramolecular Charge Transfer in the Excited State. Kinetics and Configurational Changes. *J. Photochem. Photobiol., A* **1996**, *102*, 59−70. (b) Bureš, F. Fundamental Aspects of Property Tuning in Push-Pull Molecules. *RSC Adv.* **2014**, *4*, 58826−58851.

(30) Kielesiński, Ł.; Morawski, O. W.; Barboza, C. A.; Gryko, D. T. Polarized Helical Coumarins: [1,5] Sigmatropic Rearrangement and Excited-State Intramolecular Proton Transfer. *J. Org. Chem.* **2021**, *86*, 6148−6159.

(31) (a) Yoshida, S.; Nakamura, Y.; Uchida, K.; Hazama, Y.; Hosoya, T. Aryne Relay Chemistry en Route to Aminoarenes: Synthesis of 3-Aminoaryne Precursors via Regioselective Silylamination of 3-(Triflyoxy)arynes. *Org. Lett.* **2016**, *18*, 6212−6215. (b) Corrie, J. E. T. Synthesis and Fluorescence Properties od Substituted 7-Aminocoumarin-3-carboxylate Derivatives. *J. Heterocycl. Chem.* **2000**, *37*, 1447−1455. (c) Chatterjee, A.; Seth, D. Photophysical Properties of 7-(Diethylamino)Coumarin-3-carboxylic Acid in the Nanocage of Cyclodextrins and in Different Solvents and Solvent Mixtures. *Photochem. Photobiol.* **2013**, *89*, 280−293. (d) Rettig, W.; Klock, A. Intramolecular Fluorescence Quenching in Aminocoumarins. Identification of an Excited State with Full Charge Separation. *Can. J. Chem.* **1985**, *63*, 1649−1653. (e) Krystkowiak, E.; Dobek, K.; Maciejewski, A. An Intermolecular Hydrogen-Bonding Effect on Spectral and Photophysical Properties of 6-Aminocoumarin in Protic Solvents. *Photochem. Photobiol. Sci.* **2013**, *12*, 446−455.

https://doi.org/10.1021/acs.joc.2c00232
J. Org. Chem. 2022, 87, 5961−5975

(32) Kielesiński, Ł.; Gryko, D. T.; Sobolewski, A. L.; Morawski, O. W. Effect of Conformational Flexibility on Photophysics of Bis-Comuarins. *Phys. Chem. Chem. Phys.* **2018**, *20*, 14491−14503.
(33) Kielesiński, Ł.; Gryko, D. T.; Sobolewski, A. L.; Morawski, O. The Interplay between Solvation and Stacking of Aromatic Rings Governs Bright and Dark Sites of Benzo[g]coumarins. *Chem.—Eur. J.* **2019**, *25*, 15305−15314.
(34) (a) Kim, I.; Kim, D.; Sambasivan, S.; Ahn, K. H. Synthesis of π-Extended Coumarins and Evaluation of Their Precursors as Reactive Fluorescent Probes for Mercury Ions. *Asian J. Org. Chem.* **2012**, *1*, 60−64. (b) Kim, D.; Xuan, Q. P.; Moon, H.; Jun, Y. W.; Ahn, K. H. Synthesis of Benzocoumarins and Characterization of Their Photophysical Properties. *Asian J. Org. Chem.* **2014**, *3*, 1089−1096.
(35) Ventura, B.; Poronik, Y. M.; Deperasińska, I.; Gryko, D. T. How a Small Structural Difference Can Turn Optical Properties of π-Extended Coumarins Upside Down: The Role of Non-Innocent Saturated Rings. *Chem.—Eur. J.* **2016**, *22*, 15380−15388.
(36) Singha, S.; Kim, D.; Roy, B.; Sambasivan, S.; Moon, H.; Rao, A. S.; Kim, J. Y.; Joo, T.; Park, J. W.; Rhee, Y. M.; Wang, T.; Kim, K. H.; Shin, Y. H.; Jung, J.; Ahn, K. H. A Structural Remedy Toward Bright Dipolar Fluorophores in Aqueous Media. *Chem. Sci.* **2015**, *6*, 4335−4342.
(37) Kielesiński, Ł.; Morawski, O.; Dobrzycki, Ł.; Sobolewski, A. L.; Gryko, D. TD. T. The Coumarin-Dimer Spring − The Struggle Between Charge Transfer and Steric Interactions. *Chem.—Eur. J.* **2017**, *23*, 9174−9184.
(38) (a) Chen, M. C.; Chen, D. G.; Chou, P. T. Fluorescent Chromophores Containing the Nitro Group: Relatively Unexplored Emissive Properties. *ChemPlusChem* **2020**, *86*, 11−27. (b) Rodríguez-Córdoba, W.; Gutiérrez-Arzaluz, L.; Cortés-Guzmán, F.; Peon, J. Excited State Dynamics and Photochemistry of Nitroaromatic Compounds. *Chem. Commun.* **2021**, *57*, 12218−12235. (c) Poronik, Y. M.; Sadowski, B.; Szychta, K.; Quina, F. H.; Vullev, V. I.; Gryko, D. T. Revisiting the Non-fluorescence of Nitroaromatics: Presumption versus Reality. *J. Mater. Chem. C* **2022**, *10*, 2870−2904.
(39) Frisch, M. J.; Trucks, G. W.; Schlegel, H. B.; Scuseria, G. E.; Robb, M. A.; Cheeseman, J. R.; Scalmani, G.; Barone, V.; Petersson, G. A.; Nakatsuji, H.; Li, X.; Caricato, M.; Marenich, A. V.; Bloino, J.; Janesko, B. G.; Gomperts, R.; Mennucci, B.; Hratchian, H. P.; Ortiz, J. V.; Izmaylov, A. F.; Sonnenberg, J. L.; Williams-Young, D.; Ding, F.; Lipparini, F.; Egidi, F.; Goings, J.; Peng, B.; Petrone, A.; Henderson, T.; Ranasinghe, D.; Zakrzewski, V. G.; Gao, J.; Rega, N.; Zheng, G.; Liang, W.; Hada, M.; Ehara, M.; Toyota, K.; Fukuda, R.; Hasegawa, J.; Ishida, M.; Nakajima, T.; Honda, Y.; Kitao, O.; Nakai, H.; Vreven, T.; Throssell, K.; Montgomery, J. A., Jr.; Peralta, J. E.; Ogliaro, F.; Bearpark, M. J.; Heyd, J. J.; Brothers, E. N.; Kudin, K. N.; Staroverov, V. N.; Keith, T. A.; Kobayashi, R.; Normand, J.; Raghavachari, K.; Rendell, A. P.; Burant, J. C.; Iyengar, S. S.; Tomasi, J.; Cossi, M.; Millam, J. M.; Klene, M.; Adamo, C.; Cammi, R.; Ochterski, J. W.; Martin, R. L.; Morokuma, K.; Farkas, O.; Foresman, J. B.; Fox, D. J. *Gaussian 16*, Revision A.03. Gaussian, Inc.: Wallingford CT, 2016.
(40) (a) Budzák, Š.; Charaf-Eddin, A.; Medved', M.; Gryko, D. T.; Jacquemin, D. Optical Properties of V-Shaped Bis-Coumarins: Ab Initio Insights. *Comput. Theor. Chem.* **2016**, *1076*, 57−64. (b) Xue, Y.; An, L.; Zheng, Y.; Zhang, L.; Gong, X.; Qian, Y.; Liu, Y. Structure and Electronic Spectral Property of Coumarin Chalcone Hybrids: A Comparative Study Using Conventional and Long-Range Corrected Hybrid Functionals. *Comput. Theor. Chem.* **2012**, *981*, 90−99. (c) Zhao, Y.; Truhlar, D. G. The M06 Suite of Density Functionals for Main Group Termochemistry, Thermochemical Kinetics, Noncovalent Interactions, Excited States, and Transition Elements: Two New Functionals and Systematic Testing of Four M06-Class Functionals and 12 Other Functionals. *Theor. Chem. Acc.* **2008**, *120*, 215−241.
(41) Samanta, A.; Fessenden, R. W. Excited-State Dipole Moment of 7-Aminocoumarins as Determined from Time-Resolved Microwave Dielectric Absorption Measurements. *J. Phys. Chem. A* **2000**, *104*, 8577−8582.
(42) Kapturkiewicz, A.; Herbich, J.; Karpiuk, J.; Nowacki, J. Intramolecular Radiative and Radiationless Charge Recombination Processes in Donor-Acceptor Carbazole Derivatives. *J. Phys. Chem. A* **1997**, *101*, 2332−2344.
(43) Kielesiński, Ł.; Morawski, O. W.; Sobolewski, A. L.; Gryko, D. T. The Synthesis and Photophysical Properties of Tris-Coumarins. *Phys. Chem. Chem. Phys.* **2019**, *21*, 8314−8325.
(44) Birks, J. B. *Photophysics of Aromatic Molecules*; Wiley: London, 1979; pp 97−100.
(45) Demas, J. N. *Excited State Lifetime Measurements*; Academic Press: NY, 1983; pp 89−92.
(46) Górski, K.; Deperasińska, I.; Baryshnikov, G. V.; Ozaki, S.; Kamada, K.; Ågren, H.; Gryko, D. T. Quadrupolar Dyes Based on Highly Polarized Coumarins. *Org. Lett.* **2021**, *23*, 6770−6774.

https://doi.org/10.1021/acs.joc.2c00232
J. Org. Chem. 2022, 87, 5961−5975